substance: boron compounds with group IV elements: boron carbide
property: transport properties

(see also Figs. 1, 2, 3, 4)

A review of the state of interpretation of the transport properties of icosahedral boron-rich solids in general is given in LB III/41C ("Boron"). For boron carbide is experimentally proved that at least at lower temperatures hopping is the prevailing transport mechanism. However, the discussion, how these hopping processes can be explained in detail, has remained controversy. Two basically different conceptions are presently used for the interpretation:

(i) **The hole-bipolaron hypothesis** [83E, 84E, 86E1, 87E2, 86H1, 87E2, 87E3, 87H2, 87H3, 87H1, 90E, 93E, 94E, 96E]. It is based on the assumption of hole bipolarons hopping between $B_{11}C$ icosahedra in boron carbide. The only direct experimental basis for this theory is the very low ESR spin density in boron carbide, for which several other less sophisticated reasons are available for explanation as well. Indeed, this model allowed to describe some uncommon electronic properties of boron carbide. However, it is in contrast to numerous other experimental results, even if the formation of small polarons in boron carbide cannot be excluded at all. For example, the conductivity maximum coincides with the minimum concentration of $B_{11}C$ icosahedra in the homogeneity range. In particular, this theory is not able do describe the general contribution of delocalized carriers (~10^{17}...10^{18} cm^{-3} at 300 K) to the electronic transport at lower temperatures because of the high ionization energy (> 5...6 eV) of the bipolarons (10^{21} cm^{-3}).

On the anomalous electronic transport in boron carbides see [84E].

(ii) **The semiconductor conception.** In agreement with the energy band structure calculations, this conception assumes for boron carbide an energy band structure with flat bands and accordingly high effective masses ($m^* \approx$ 5...10 m_0) and low mobilities of the delocalized carriers ($\mu \approx$ 30...330 $cm^2V^{-1}s^{-1}$). The main contribution to the charge transport comes from localized carriers (polarons?) with low mobilities ($\mu \approx 3$ $cm^2V^{-1}s^{-1}$) hopping between certain localized states in the band gap (see Fig. 5). It has been shown that the localized states in the band gap of boron carbide are evoked by defects in the structure, that are required to compensate the valence electron deficiency, which is theoretically calculated for idealized structures [99S3, 99S4, 99S5]. At least most of the experimental results, which have become known can be consistently described within this conception.

A further model proposed to describe the electronic transport in icosahedral boron-rich solids, the "amorphous concept" (see [83G, 87G, 91G] and LB III/41C) is based on the assumption that in the boron-rich solids an amorphization exists, whose degree depends on the number of atoms per unit cell. However, this conception completely fails for boron carbide, whose number of atoms per unit cell is comparably low in the sense of this conception, but whose electronic properties are strongly "amorphous-like".

transport theory

Small-polaron electronic transport in boron carbides [83E].

Quasi-localization and electronic transport in boron and boron-rich borides [86B].

Small bipolaronic hopping in boron carbides [86E1].

Conduction mechanism in boron carbide [84W3].

Electronic transport in boron carbides [86E1].

Polaron formation in systems of boron icosahedra [86H2].

Electronic transport in icosahedral boron-rich solids (in particular boron carbide) in [87E3].

Bipolarons in boron icosahedra [87H5].

Bipolaron formation in B_{12} and $B_{11}C$ icosahedra [87H4].

Theory of electronic and thermal transport in boron carbides [90E] . (The paper contains experimental results on electrical conductivity, Hall mobility and thermal diffusivity).

Electronic and vibrational transport in boron carbides [91E1].

Effects of disorder on self-trapping and subsequent hopping in boron carbides [94E].

dc conductivity

electrical conductivity

(in $\Omega^{-1}cm^{-1}$)

σ	$2.5 \cdot 10^{-4}$	T = 77 K	single crystal, nearly $B_{4.3}C$	87W3
	$5 \cdot 10^{-1}$	T = 290 K		93S
	11	T = 295 K	~ 10 at. % C (see Fig. 6)	

22		~ 13.2 at. % C	
12		~ 15.5 at. % C	
5		~ 18 at. % C	
3		~ 18.6 at. % C	
3.5		~ 20 at. % C	
1.4...12	T = 300 K	value depends on C content (cf. Fig. 1)	80W, 81W3
$8 \cdot 10^{-2}$...5	T = 100 K	value depends on C content	

See also [70G2, 79B2, 79T, 79K2].

For temperature dependence, see Fig. 2.

Activation energy of the electrical conductivity and Peltier energy: Figs. 7, 8.

hopping energy E_h and $a^2\nu$ for CVD boron carbide

(from Hall mobility; (a, hopping distance; ν, hopping frequency)

Composition	E_h [eV]	$a^2\nu$ [cm^2s^{-1}]	
B_4C	0.13	23.6	94K1
$B_{5.54}C$	0.13	15.3	
$B_{6.57}C$	0.12	8.0	
$B_{9.62}C$	0.12	9.9	

Electrical conductivity vs. B/C relation and temperature in Fig. 9 [90W2, 94K3, 99W].

Electrical conductivity of different compounds within the homogeneity range for temperatures between about 5 and 2200 K plotted in Fig. 10 according to Mott's law for variable-range hopping:

$\sigma = \sigma_0 \exp -(T_0/T)^{1/4}$

with $T_0 = (2.1)^4\ \alpha^3/N(E_F)k_B$, and

$\sigma_0 = e^2/[2(8\pi)^{1/2}] \cdot f_{phonon} \cdot [N(E_F)/(\alpha k_B T)]^{1/2}$

with α: reciprocal localization length, f_{phonon}: phonon frequency.

High temperature electrical conductivity versus reciprocal temperature in Fig. 11 [86W2. 87W4, 90W2, 91W, 98W, 99W].

According to Abrahams et al. [79A] and Möbius [85M] can be checked, whether a unique conductivity mechanism exists in a system of compounds, even if the determining parameters of the system like e.g. the chemical composition are modified. A scaling behavior of hopping systems is determined by the functional relation between conductivity and microscopic parameters $\sigma \sim \sigma_0\ \beta[T/T_0(\alpha, x, R, ...)]$ (α^{-1}, localization length; x, composition; R, distance between localized states). The plot of $d \log\sigma/dT$ vs. $\log(\sigma^{-1})$ for numerous boron carbide samples in Fig. 12 [99W, 80W, 81W3, 90N, 91W]: confirms that for boron carbide this is largely the case independent of chemical composition, temperature and preparation technique.

Anisotropy of the electrical conductivity in Fig. 13 [86W4]. The small anisotropy disproves the conception of covalent bonding || *c* and metallic bonding ⊥ *c* [76W, 79K2, 80K].

Pressure dependence of the electrical conductivity of B_4C at 297 and 425 K, B_9C at 300 K in Fig. 14 [85S].

Temperature dependence of the electrical conductivity of boron carbide (B_4C) vs. reciprocal *T* for different pressures in Fig. 15 [85S].

I(*U*) plot for an approximately $B_{4.3}C$ single crystal (see Fig. 13) in Fig. 16 [86W4].

Dependence of the dc and high frequency electrical conductivity on the carbon content in Fig. 17 [90W2, 80W, 81W3, 86W1, 97S, 98W].

Low temperature dc conductivity and minimum hopping rate in Fig. 18 [91Z].

Electrical resistivity (and ESR) in [80V].

Electrical conductivity, thermoelectric power, Hall mobility, activation energy dependence on composition; metal-semiconductor transition [81W3].

Temperature dependence of the electrical conductivity for different compositions [85B].

Anisotropy of the electrical conductivity, activation energy of the electrical conductivity in [86W4].

High temperature resistivity in [86W5].

Effect of thermal cycling on resistivity and Seebeck effect in Fig. 19 [86W5].

Electrical conductivity and Hall mobility in [87E3, 86E3].

Electrical conductivity, Hall effect, Seebeck effect, structure dependence, dependence on thermal cycling in [86W1].

Temperature dependence of the electrical conductivity of $B_{13}C_2$ in [86W1].

dc conductivity, ac conductivity, Seebeck, dielectric function in [86K].

Resistivity depending on temperature in [87W4].

Heating-cooling cycles of conductivity and Hall effect in [87W4].

Low temperature electrical conductivity according to Mott's law in [90W1].

High temperature electrical conductivity of B_xC (x =3,4, 5) [91M].

Electrical conductivity depending on composition in [94A].

Isothermes of the electrical conductivity dependence. on composition in [94A].

Electrical conductivity of boron carbide depending on temperature and carbon content in [94K3].

Transport properties of boron carbide (conductivity, . Hall constant, Hall mobility vs. 1/*T*) in [95A].

Comment on the metal-insulator transition in boron carbide (Fig. 1) [80W, 81W3]: The metal-insulator transition was found within the homogeneity range at carbon contents close to the carbon-rich limit, which was assumed to be B_4C at that time. Meanwhile is known that the carbon-rich limit of the homogeneity range is $B_{4.3}C$ in reality. Accordingly, the compounds between both compositions contain certain amounts of excess carbon, which is probably responsible for the metal-insulator transition, and may exist in the structure in atomic distribution. Since metal-like conductivity was found at low temperatures only, carbon precipitation in the form of graphitic layers known from higher amounts of excess carbon can be largely excluded.

ac conductivity

(in $\Omega^{-1}cm^{-1}$)

σ	2.4(6)	T = 295 K	~ 10 at. % C, 10^{10} Hz	93S
	7.0(10)		~ 13.2 at. % C, 10^{10} Hz	
	2.0(6)		~ 15.5 at. % C, 10^{10} Hz	
	1.0(2)		~ 18 at. % C, 10^{10} Hz	
	1.1(2)		~ 20 at. % C, 10^{10} Hz	

ac conductivities of undoped and p-doped boron carbide between 10^3 and 10^6 Hz in Fig. 20 [93A].

Electrical conductivity for 10^{10} Hz compared with dc results vs. carbon concentration in Fig. 21 (=Fig. 6) [93S].

Frequency dependence of the ac conductivity of $B_{4.5}C$ at T = 4 K and $B_{9.0}C$ at T =4,10, and 15 K; temperature dependence of the power-law dependence on frequency for B_9C in Fig. 22 [93S].

Temperature dependence of the electrical conductivity of $B_{4.5}C$ and B_9C for frequencies between 10^3 and 10^6 Hz in Fig. 23 [93S].

Frequency dependence of the electrical conductivity for $B_{4.3}C$ (8, 22 and 46 K) and $B_{13}C_2$ (4, 10 and 40 K) in Fig. 24 [91Z].

Frequency dependence of the electrical conductivity of $B_{1-x}C_x$ (x = 0.2...0.13) at 4.2 K in Fig. 25 [86K].

Temperature dependence of the electrical conductivity for frequencies up to 10^9 Hz in Fig. 26 [86K].

dynamical conductivity

In consequence of the dynamical conductivity the reflectivity in the FIR spectral range increases towards lower wave numbers. In earlier investigations ([73B, 79B2, 87W1, 87W2, 90W1] see also Fig. 27) this behavior was attributed to strongly damped Drude-type free carriers. Recent investigations have shown that a satisfactory quantitative description of the experimental results is only possible, when a superposition of hopping-type and Drude-type electronic transport is assumed [96S, 97S, 98S, 99S1]. Indeed, under specific conditions the transport of delocalized Drude-type carriers can be below the detection limit. For spectra see below.

Density of delocalized holes vs. reciprocal T derived from the dynamical conductivity of $B_{6.3}C$ and $B_{7.91}C$ (optical spectra) [98S, 99S1] compared with the Hall densities determined from Hall effect and magnetoresistance of $B_{4.3}C$ single crystals [85W, 87W3]. and compared with model calculations (i) taking the density of unoccupied atomic sites in the structure into account and (ii) based on an ideal structure without vacancies in Fig. 28 [98S, 99S1].

photoconductivity

Prove of the electron-phonon interaction in $B_{10.37}C$ by the change of the oscillator strength of the ~1080 cm^{-1} IR-active phonon by the optical excitation of carriers [93W, 94K2].

Drude-type optical absorption of optically excited carriers in $B_{10.37}C$ [97W].

Interaction of optically excited carriers with intra-icosahedral phonons in Fig. 29 [97W].

Hall effect

Hall coefficient
(in cm^3C^{-1})

R_H	0.08	T = 300 K	$B_{13}C_2$	86W1
	0.06		$B_{15}C_2$	87W4
	0.12		$B_{\sim 4.3}C$ (ESK boron carbide)	
	(– 4...+ 19) $\cdot 10^{-2}$	T = 300K	value depends on C content, see Fig. 30	80W

hole mobility
(in $cm^2V^{-1}s^{-1}$)

$\mu_{H,p}$	37	T = 77 K	Hall effect, single crystal, $B_{\sim 4.3}C$ (ESK boron carbide)	87W3
	20		magnetoresistance, single crystal	
	0.8	T = 290K	Hall effect, single crystal	
	1		magnetoresistance, single crystal	
	2.5	T = 300 K	$B_{13}C_2$	86W1
	~2		$B_{15}C_2$	87W4
	~2		$B_{\sim 4.3}C$ (ESK boron carbide)	
	0.2...1	T = 300 K	Hall effect, ESR, conductivity	70G2, 77G

hole concentration

p	$2.1 \cdot 10^{13}$ cm^{-3}	T = 77 K	from Hall effect and el. cond., ~$B_{4.3}C$	87W3
	$3.9 \cdot 10^{17}$ cm^{-3}	T = 290 K	(ESK boron carbide)	
	$(4...9) \cdot 10^{19}$ cm^{-3}	T = 300 K	Hall effect, ESR	70G2, 77G

Dependence of the Hall effect on the composition for15, 220, 400, 550 and 700 °C in Fig. 31 [86W5].

Temperature dependence of the Hall coefficient of $B_{4.1}C$ (close to the carbon-rich limit of the homogeneity range), $B_{3.1}C$ (with excess carbon) and $B_{8.3}C$ in Fig. 32 [90W2, 91W].

Temperature dependence of the Hall effect in a heating-cooling cycle in Fig. 33 [86W1, 86W5, 87W4].

Temperature dependence of the Hall mobility of boron carbide in Fig. 34 [70G2, 86W1, 86W5, 87W4, 90W2, 91W, 96C].

Change of sign of the Hall effect (Hall coefficient and Hall mobility) of $B_{11}C$ prepared by CVD at 140 °C in Fig. 35 [87C].

Temperature dependence of the Hall mobility of CVD boron carbide for $B_{4.00}C$, $B_{5.54}C$, $B_{6.57}C$ and $B_{9.62}C$ in Fig. 36 [94K1].

Hall mobility and electrical conductivity in [89A].

Electrical conductivity and Hall mobility in [87E1, 87E2].

Hall effect in [87W4, 90W1].

Linear dependence of the Hall voltage up to B = 15 T in [87W3, 90W1, 91W].

magnetoresistance

Dependence of the magnetoresistance on B (B up to 15 T) at 77 and 290 K in Fig. 37 [87W3, 90W1, 91W].

Seebeck effect

The amount of the Seebeck coefficient (thermoelectric power) S of boron carbide ($S \sim 300\ \mu V\ K^{-1}$) is typical for semiconductors; however its temperature dependence is very unusual. While in classical semiconductors S decreases towards high temperatures because the contributions of electrons and holes largely cancel one another in the intrinsic region, the Seebeck coefficient of boron carbide remains high, up to temperatures $T > 2000$ K. This makes boron carbide a very promising candidate for high-efficiency high-temperature thermoelectric energy conversion (see [86W5, 88W, 95W]) because the figure of merit $z = S^2\sigma/\kappa$ (σ, electrical conductivity; κ, thermal conductivity) is proportional to the square of S. While most of the experimental results indicate that (i) S increases monotonically with T (see below), in others (ii) a maximum around 250 K is followed towards higher temperatures by a somewhat lower minimum at about 700 K [98A]. The behavior (i) has been only qualitatively explained by E_F being pinned up to high temperatures in high-density gap states close to the valence band. The slope (ii) was explained by a large enhancement of the Seebeck coefficient of boron carbide through vibrational softening in consequence of the strong electron-phonon interaction [98A, 98E, 99E]. In this case, as shown in Fig. 38 [99E] one enhancement is due to localized carriers inducing an increase in the solid's vibrational entropy. The other contribution is proportional to the vibrational energy transferred with the carriers as they hop.

Overview of typical results of the thermoelectric power as a function of temperature for various chemical compositions $B_{4.1}C$, $B_{4.3}C$, $B_{6.2}C$, $B_{6.9}C$ [91W], $B_{4.3}C$ anisotropy ($\|c$ and $\perp c$) [86W3, 86W4], see also [95W], B_4C, B_9C [86W1, 86W5], $B_{69}C_{11}Si$ [94W], 10 % P-doped boron carbide [94A] in Fig. 39.

thermoelectric power

S	15...160 $\mu V\ K^{-1}$	T = 300 K	value depends on C content, cf. Fig. 3	80W, 81W3

Temperature dependence of the thermoelectric power of CVD boron carbide with the compositions $B_{4.00}C$, $B_{4.95}C$, $B_{5.54}C$, $B_{6.57}C$, $B_{9.62}C$ and $B_{10.67}C$ discussed in relation to the transport properties in general in Fig. 40 [94K1].

Temperature dependence of the Seebeck coefficient of $B_{6.5}C$; comparison of experimental results and theory, based on the enhancement through vibrational softening in Fig. 41 [98A].

Temperature dependence of the Seebeck cofficient of boron carbide with 13.0, 16.4, 17.5 and 19.5 at.% C in Fig. 42 [98A].

Dependence of the Seebeck coefficient on the carbon concentration in Fig. 43 [98A].

Thermoelectric power in [87E3].

Seebeck effect in context with the transport properties in [87W4].

Thermoelectric power and figure of merit, dependence on composition for different T in [85B].

Review on high-temperature thermoelectric properties in [91A].

Thermoelectric power as a function of T in [89A].

The correlation between the thermoelectric properties and stoichiometry in the boron carbide phase B_4C – $B_{10.5}C$ [85B].

High temperature thermoelectric power in [87A].

Seebeck effect vs. T (300...1400 K) in Fig. 19 [86W5].

Calculation of the thermoelectric power of boron carbide as a function of temperature with and without extensive twinning boundaries [87E2].

B_4C/C thermocouple for high temperatures [85H, 85A].

Materials for thermoelectric energy conversion [84W1, 84W2, 88W].

Boron-rich solids: a chance for high-efficiency high-temperature thermoelectric energy conversion [95W].

Preparation and verification of boron-carbide-based thermoelectric alloy [86E2].

Refractory semiconductors for high temperature thermoelectric energy conversion [87W5].

Temperature control of inert gas furnace by B_4C/C thermocouple [88K].

References:

70G1 Gurr, G.E., Montgomery, P.W., Knutson, C.D., Gorres, B.T.: Acta Crystallogr. B 26 (1970) 906.

70G2 Geist, D., Meyer, J., Peußner, H.: in: Boron 3, T. Niemyski ed., PWN: Warsaw, 1970, p. 207.

71W Werheit, H., Binnenbruck, H., Hausen, A.: Phys. Status Solidi (b) 47 (1971) 153.

73B Binnenbruck, H.: Thesis, University of Cologne, Germany, 1973.

76W Will, G., Kossobutzki, K.H.: J. Less-Common Met. 47 (1976) 33.

77B Berezin, A. A., Golikova, O. A., Zaitsev, V. R., Kazanin, M. M., Orlov, V. M., Tkalenko, E. N., in:Boron and Refractory Borides, (Matkovich V. 1., ed.) Springer: Berlin, Heidelberg, New York 1977, p. 52.

77G Geist, D.: see [77B], p. 65.

79A Abrahams, E., Anderson, P.W., Licciardelle, D.C., Ramakrishnan, T.V: Phys. Rev. Lett. 42 (1979) 673.

79B1 Binneabruck, H., Werheit, H.: Z. Naturforsch. 34a (1979) 787.

79B2 Beauvy, M., Thevenot, F.: L'Industrie Ceramique 732 (1979) 734.

79K1 Kirfel, A., Gupta, A., Will, G.: Acta Crystallogr. B 35 (1979) 1052.

79K2 Kuzenkova, M. A., Kishyi, P. S., Grabchuk, B. L., Bodnaruk, N. I.: J. Less-Common Met. 67 (1979) 217.

79T Thevenot, F., Bouchacourt, M.: L'Industrie Ceramique 732 (1979) 655.

80K Kirfel, A., Will, G.: Acta Crystallogr. B 36 (1980) 1311.

80V Vlasova, M.V., Kakazey, N.G., Kosolapova, T.Y., Makarenko, G.N., Marek, E.V., Usokovic, D., Ristic, M.M.: J. Mater. Sci. 15 (1980) 1041.

80W Werheit, H., de Groot, K.: Phys. Status Solidi (b) 97 (1980) 229.

81A Armstrong, D. R.: Proc. 7th Int. Symp. Boron, Borides and Related Compounds. Uppsala, Sweden, 1981; spec. issue of J. Less-Common Met. 82 (1981) 357.

81W1 Werheit, H., de Groot, K., Malkemper, W., Lundström, T.: see [81A1], p. 163.

81W2 Werheit, H., Lundström, T., unpublished results.

81W3 Werheit, H., de Groot, K., Malkemper, W.: see [81A], p. 153.

83E Emin, D., Wood, C.: in: Proc. 18th Intersoc. Energy Convers. Eng. Conf., August 21-26, 1983, p. 222.

83G Golikova, O.A., Samatov, S.: Phys. Status Solidi (a) 77 (1983) 449.

84E Emin, D., Samara, G.A., Wood, C.: Anomalous Electronic Transport in Boron Carbides, in Semiconductor Conf. (8/84), San Francisco, 1984.

84W1 Wood, C.: Energy Convers. Manage. 24 (1984) 331.

84W2 Wood, C.: Energy Convers. Manage. 24 (1984) 317.

84W3 Wood, C., Emin, D.: Phys. Rev. B 29 (1984) 4582.

85A Anonymus : Sprechsaal 118 (1985) 1196.

85B Bouchacourt, M., Thévenot, F.: J. Mater. Sci. 20 (1985) 1237.

85H Hunold, K.: Chem. Tech. 14 (1985) 82.

85M Möbius, A.: J. Phys. C: Solid State Phys. 18 (1985) 3337.

85S Samara, G.A., Emin, D., Wood, C.: Phys. Rev. B 32 (1985) 2315.

85W Werheit, H., Franz, R., Schneider, D., Wolf, M., Brann, G.: in: Wissenschaftliche Berichte HMFA Braunschweig, D. Schneider ed., HMFA Braunschweig: Braunschweig, 1985, p. 53.

86B Berezin, A.A.: in: Boron-Rich Solids (AIP Conf. Proc. 140), Albuquerque, New Mexico 1985, D. Emin, T.L. Aselage, C.L. Beckel, I.A. Howard ed., American Institute of Physics: New York, 1986, p. 224.

86E1 Elsner, N.B., Reynolds, G.H., Norman, J.H., Shearer, C.H.: in: Boron-Rich Solids (AIP Conf. Proc. 140), Albuquerque, New Mexico 1985, D. Emin, T.L. Aselage, C.L. Beckel, I.A. Howard ed., American Institute of Physics: New York, 1986, p. 59.

86E2 Emin, D.: in: Boron-Rich Solids (AIP Conf. Proc. 140), Albuquerque, New Mexico 1985, D. Emin, T.L. Aselage, C.L. Beckel, I.A. Howard ed., American Institute of Physics: New York, 1986, p. 189.

86E3 Emin, D., Samara, G.A., Azevedo, L.J., Venturini, E.L., Madden, H.H., Nelson, G.C., Shelnutt, J.A., Morosin, B., Moss, M.: J. Less-Common Met. 117 (1986) 415 (Proc. 8th Int. Symp. Boron, Borides, Carbides, Nitrides and Rel. Compounds, Tbilisi, Oct. 8 - 12, 1984).
86H1 Higashi, I., Lundström, T., Kasaya, M., Kasuya, T: J. Less-Common Met. 120 (1986) L7.
86H2 Howard, I.A., Beckel, C.L., Emin, D.: in: Boron-Rich Solids (AIP Conf. Proc. 140), Albuquerque, New Mexico 1985, D. Emin, T.L. Aselage, C.L. Beckel, I.A. Howard ed., American Institute of Physics: New York, 1986, p. 240.
86K Kormann, R., Zuppiroli, L.: in: Boron-Rich Solids (AIP Conf. Proc. 140), Albuquerque, New Mexico 1985, D. Emin, T.L. Aselage, C.L. Beckel, I.A. Howard ed., American Institute of Physics: New York, 1986, p. 216.
86W1 Wood, C.: in: Boron-Rich Solids (AIP Conf. Proc. 140), Albuquerque, New Mexico 1985, D. Emin, T.L. Aselage, C.L. Beckel, I.A. Howard ed., American Institute of Physics: New York, 1986, p. 206.
86W2 Werheit, H., Franz, R., Higashi, I.: J. Less-Common Met. 117 (1986) 169 (Proc. 8th Int. Symp. Boron, Borides, Carbides, Nitrides and Rel. Compounds, Tbilisi, Oct. 8 - 12, 1984).
86W3 Werheit, H., Kemper, D.: (unpublished results).
86W4 Werheit, H., Rospendowski, S.: in: Boron-Rich Solids (AIP Conf. Proc. 140), Albuquerque, New Mexico 1985, D. Emin, T.L. Aselage, C.L. Beckel, I.A. Howard ed., American Institute of Physics: New York, 1986, p. 234.
86W5 Wood, C.: in: Boron-Rich Solids (AIP Conf. Proc. 140), Albuquerque, New Mexico 1985, D. Emin, T.L. Aselage, C.L. Beckel, I.A. Howard ed., American Institute of Physics: New York, 1986, p. 362.
87A Aselage, T.L., Emin, D., Wood, C., Mackinnon, I.D.R., Howard, I.A.: in: Novel Refractory Semiconductors, MRS Symp. Proc. Vol. 97, D. Emin, T.L. Aselage, C. Wood ed., Materials Research Soc.: Pittsburgh, 1987, p. 27.
87C Campbell, A.N., Mullendore, A.W., Tallant, D.R., Wood, C.: in: Novel Refractory Semiconductors, MRS Symp. Proc. Vol. 97, D. Emin, T.L. Aselage, C. Wood ed., Materials Research Soc.: Pittsburgh, 1987, p. 113.
87E1 Emin, D.: in: Novel Refractory Semiconductors, MRS Symp. Proc. Vol. 97, D. Emin, T.L. Aselage, C. Wood ed., Materials Research Soc.: Pittsburgh, 1987, p. 3.
87E2 Emin, D.: Physics Today January (1987) 55.
87E3 Emin, D.: in: Proc. 9th Int. Symp. Boron, Borides and Rel. Compounds, University of Duisburg, Germany, Sept. 21 - 25, 1987, H. Werheit ed., University of Duisburg: Duisburg, 1987, p. 154.
87G Golikova, O.A.: in: Novel Refractory Semiconductors, MRS Symp. Proc. Vol. 97, D. Emin, T.L. Aselage, C. Wood ed., Materials Research Soc.: Pittsburgh, 1987, p. 17.
87H1 Higashi, I., Ito, T.: in: Proc. 9th Int. Symp. Boron, Borides and Rel. Compounds, University of Duisburg, Germany, Sept. 21 - 25, 1987, H. Werheit ed., University of Duisburg: Duisburg, 1987, p. 41.
87H2 Higashi, I., Kasaya, M., Okabe, A., Kasuya, T.: J. Solid State Chem. 69 (1987) 376.
87H3 Higashi, I., Sida, J., Iimura, Y., Takahashi, Y.: in: Proc. 9th Int. Symp. Boron, Borides and Rel. Compounds, University of Duisburg, Germany, Sept. 21 - 25, 1987, H. Werheit ed., University of Duisburg: Duisburg, 1987, p. 271.
87H4 Howard, I.A., Beckel, C.L., Emin, D.: in: Novel Refractory Semiconductors, MRS Symp. Proc. Vol. 97, D. Emin, T.L. Aselage, C. Wood ed., Materials Research Soc.: Pittsburgh, 1987, p. 39.
87H5 Howard, I.A., Beckel, C.L., Emin, D.: Phys. Rev. B 35 (1987) 2929.
87W1 Werheit, H.: in: Proc. 9th Int. Symp. Boron, Borides and Rel. Compounds, University of Duisburg, Germany, Sept. 21 - 25, 1987, H. Werheit ed., University of Duisburg: Duisburg, 1987, p. 142.
87W2 Werheit, H., Haupt, H.: Z. Naturforsch. 42a (1987) 925.
87W3 Werheit, H., Franz, R., Schneider, D., Wolf, M., Brann, G.: in: Proc. 9th Int. Symp. Boron, Borides and Rel. Compounds, University of Duisburg, Germany, Sept. 21 - 25, 1987, H. Werheit ed., University of Duisburg: Duisburg, 1987, p. 381.
87W4 Wood, C.: in: Proc. 9th Int. Symp. Boron, Borides and Rel. Compounds, University of Duisburg, Germany, Sept. 21 - 25, 1987, H. Werheit ed., University of Duisburg: Duisburg, 1987, p. 213.
87W5 Wood, C.: in: Novel Refractory Semiconductors, MRS Symp. Proc. Vol. 97, D. Emin, T.L. Aselage, C. Wood ed., Materials Research Soc.: Pittsburgh, 1987, p. 335.
88K Kanno, Y.: Report Government Industrial Research Institute (1988) (unpublished report (via ESK)).
88W Wood, C.: Rep. Prog. Phys. 51 (1988) 51.
89A Aselage, T., Emin, D., Wood, C.: in: Trans. 6th Symp. on Space Nuclear Power, Albuquerque, NM, Jan. 8 - 12, 1989, p. 430.
90E Emin, D.: in: The Physics and Chemistry of Carbides, Nitrides and Borides; NATO ASI Series E: Applied Sciences Vol. 185, R. Freer ed., Kluwer Academic Publishers: Dordrecht, 1990, p. 691.
90N Nair, K.U., Werheit, H., Winkelbauer, W.: (1990) unpublished results

90W1 Werheit, H.: in: The Physics and Chemistry of Carbides, Nitrides and Borides; NATO ASI Series E: Applied Sciences Vol. 185, R. Freer ed., Kluwer Academic Publishers: Dordrecht, 1990, p. 677.
90W2 Werheit, H., Herstell, B., Winkelbauer, W.: (unpublished results)).
91A Aselage, T.L.: in: Modern perspectives on thermoelectrics and related materials symposium, Anaheim, Allred, D.D., Vining C.B, Slack G.A., Pittsburgh P.A. ed., Materials Research Soc.: 1991, p. 145.
91E1 Emin, D.: in: Boron-Rich Solids, Proc. 10th Int. Symp. Boron, Borides and Rel. Compounds, Albuquerque, NM 1990 (AIP Conf. Proc. 231), D. Emin, T.L. Aselage, A.C. Switendick, B. Morosin, C.L. Beckel ed., American Institute of Physics: New York, 1991, p. 65.
91E2 Etourneau, J.R.: in: Inorganic reactions and methods, J.J. Zuckerman, A.P. Hagen ed., VCH, Publishers Inc.: New York, 1991, p. 203.
91G Golikova, O.A.: in: Boron-Rich Solids, Proc. 10th Int. Symp. Boron, Borides and Rel. Compounds, Albuquerque, NM 1990 (AIP Conf. Proc. 231), D. Emin, T.L. Aselage, A.C. Switendick, B. Morosin, C.L. Beckel ed., American Institute of Physics: New York, 1991, p. 108.
91M Matsui, T., Arita, Y., Naito, K., Imai, H.: J. Nucl. Mater. 186 (1991) 7.
91W Werheit, H., Kuhlmann, U., Franz, R., Winkelbauer, W., Herstell, B., Fister, D., Neisius, H.: in: Boron-Rich Solids, Proc. 10th Int. Symp. Boron, Borides and Rel. Compounds, Albuquerque, NM 1990 (AIP Conf. Proc. 231), D. Emin, T.L. Aselage, A.C. Switendick, B. Morosin, C.L. Beckel ed., American Institute of Physics: New York, 1991, p. 104.
91Z Zuppiroli, L., Papandreou, N., Kormann, R.: J. Appl. Phys. 70 (1991) 246.
93A Aselage, T.L., Emin, D., Samara, G.A., Tallant, D.R., van Deusen, S.B., Eatough, M.O., Tardy, H.L., Venturini, E.L.: Phys. Rev. B 48 (1993) 11759.
93E Emin, D.: Phys. Rev. B 48 (1993) 13691.
93S Samara, G.A., Tardy, H.L., Venturini, E.L., Aselage, T.L., Emin, D.: Phys. Rev. B 48 (1993) 1468.
93W Werheit, H., Kuhlmann, U.: Solid State Commun. 88 (1993) 21.
94A Aselage, T.L., Tallant, D.R., Emin, D., van Deusen, S.B., Yang, P.: Proc. 11th Int. Symp. Boron, Borides and Rel. Compounds, Tsukuba, Japan, August 22 - 26, 1993, Jpn. J. Appl. Phys. Series 10 (1994), p. 58.
94E Emin, D.: Proc. 11th Int. Symp. Boron, Borides and Rel. Compounds, Tsukuba, Japan, August 22 - 26, 1993, Jpn. J. Appl. Phys. Series 10 (1994), p. 62.
94K1 Koumoto, K.: Am. Ceram. Soc. Bull. 73 (1994) 84.
94K2 Kuhlmann, U.: Zusammenhänge zwischen den Phononenspektren borreicher Festkörper mit Ikosaederstruktur und ihren strukturellen und elektronischen Eigenschaften, Thesis, Gerhard-Mercator University, Duisburg, Germany, 1994.
94K3 Kuhlmann, U., Werheit, H.: Proc. 11th Int. Symp. Boron, Borides and Rel. Compounds, Tsukuba, Japan, August 22 - 26, 1993, Jpn. J. Appl. Phys. Series 10 (1994), p. 84.
94W Werheit, H., Kuhlmann, U., Laux, M., Telle, R.: J. Alloys Compounds 209 (1994) 181.
95A Aselage, T.L., Emin, D.: in: CRC Handbook of Thermoelectrics, Rowe D.M. ed., CRC Press: Boca Raton, 1995, p. 373.
95W Werheit, H.: Mater. Sci. Eng. 29 (1995) 228, High Temperature Electronics, EMRS Symp. Proc. 50 (1994); Mater. Sci. Eng. B29, K. Fricke and V. Krozer ed., North Holland: Amsterdam, 1995, p. 228.
96C Chauvet, O., Emin, D., Forro, L., Aselage, T.L., Zuppiroli, L.: Phys. Rev. B 53 (1996) 14450.
96E Emin, D.: Phys. Rev. B 53 (1996) 1260.
96S Schmechel, R., Werheit, H.: J. Phys.: Condens. Matter 8 (1996) 7263.
97K Kawai, J., Muramatsu, Y., Agui, A., Shin, S., Kato, H.: Spectrochim Acta B 52 (1997) 593.
97S Schmechel, R., Werheit, H.: J. Solid State Chem. 133 (1997) 335 (Proc. 12th Int. Symp. Boron, Borides and Rel. Compounds, Baden, Austria, Aug. 25 - 30, 1996).
97W Werheit, H., Schmechel, R., Lorse, K.P.: J. Solid State Chem. 133 (1997) 125,(Proc. 12th Int. Symp. Boron, Borides and Rel. Compounds, Baden, Austria, Aug. 25 - 30, 1996).
98A Aselage, T.L., Emin, D., McCready, S.S., Duncan, R.V.: Phys. Rev. Lett. 81 (1998) 2316.
98E Emin, D.: Phys. Status Solidi (b) 205 (1998) 385.
98S Schmechel, R.: Thesis, Gerhard-Mercator University Duisburg, Germany, 1998.
98W Werheit, H.: in: Materials Science of Carbides, Nitrides and Borides (Proc. NATO ASI on "Materials science of carbides, nitrides and borides", St. Petersburg, Russia, August 12-22, 1998), Y.G. Gogotsi, R.A. Andrievski ed., Kluwer Academic Publishers, 1998, p. 65.
99E Emin, D.: Phys. Rev . B 59 (1999) 6205.
99S1 Shirai, K., Katayama-Yoshida, H.: J. Solid State Chem. (2000) (Proc. 13th Int. Symp. Boron, Borides and Rel. Compounds, Dinard, France, Sept. 1999).
99S2 Shitsevalova, N., Czopnik, A., Paderno, Yu.B., Krivchikov, A., Pietrasko, A., Pluzhnikov, V.: J. Solid State Chem. (2000) (Proc. 13th Int. Symp. Boron, Borides and Rel. Compounds, Dinard, France, Sept. 1999).
99S3 Schmechel, R., Werheit, H.: J. Phys.: Condens. Matter 11 (1999) 6803.

99S4 Schmechel, R., Werheit, H.: J. Solid State Chem. (2000) (Proc. 13th Int. Symp. Boron, Borides and Rel. Compounds, Dinard, France, Sept. 1999: Structural defects of icosahedral boron-rich solids and their correlation with the electronic properties).

99S5 Schmechel, R., Werheit, H.: J. Solid State Chem. (2000) (Proc. 13th Int. Symp. Boron, Borides and Rel. Compounds, Dinard, France, Sept. 1999: Photoluminescence of high-purity b-rhombohedral boron and of boron carbide).

99W Werheit, H.: in: Electric Refractory Materials, Y. Kumashiro ed., Marcel Dekker: New York, 1999 (in press).

99Z Zaoui, A., Certier, M., Ferhat, M., Paés, O., Aourag, H.: Phys. Status Solidi (b) 212 (1999) 307.

Fig. 1.

Boron carbide. Transport properties and resonance wavenumber of the 1080 cm^{-1} phonon vs. medium distance of the C atoms. The compositions $B_{12}C_3$ and $B_{13}C_2$ are outlined [81W1].

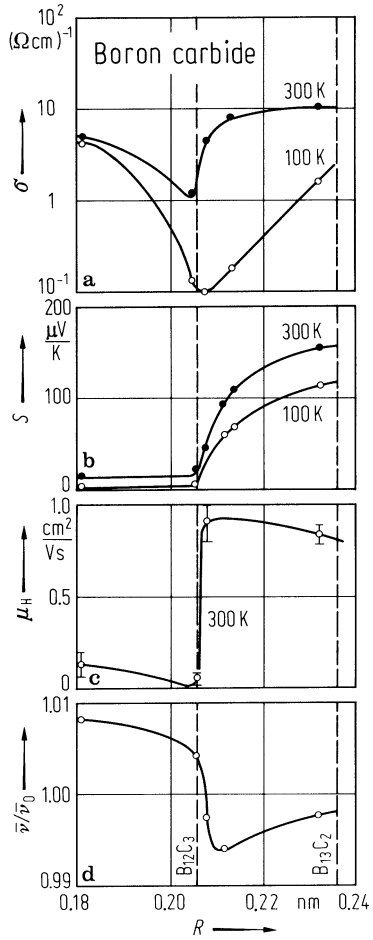

Fig. 2.

Boron carbide. a) Electrical conductivity vs. reciprocal temperature. For sample composition, see Fig. 8b. Electrical conductivity vs. $T^{-1/4}$ (according to Mott's law) [80W, 81W2].

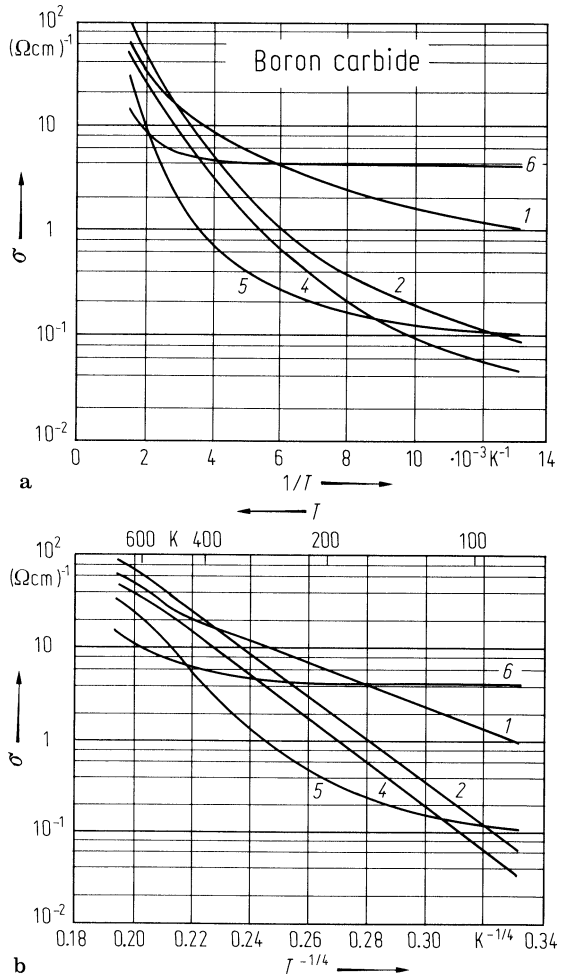

Fig. 3.

Boron carbide. a) Thermoelectric power vs. temperature. For sample composition, see Fig. 8b. Thermoelectric power vs. reciprocal temperature [80W, 81W2].

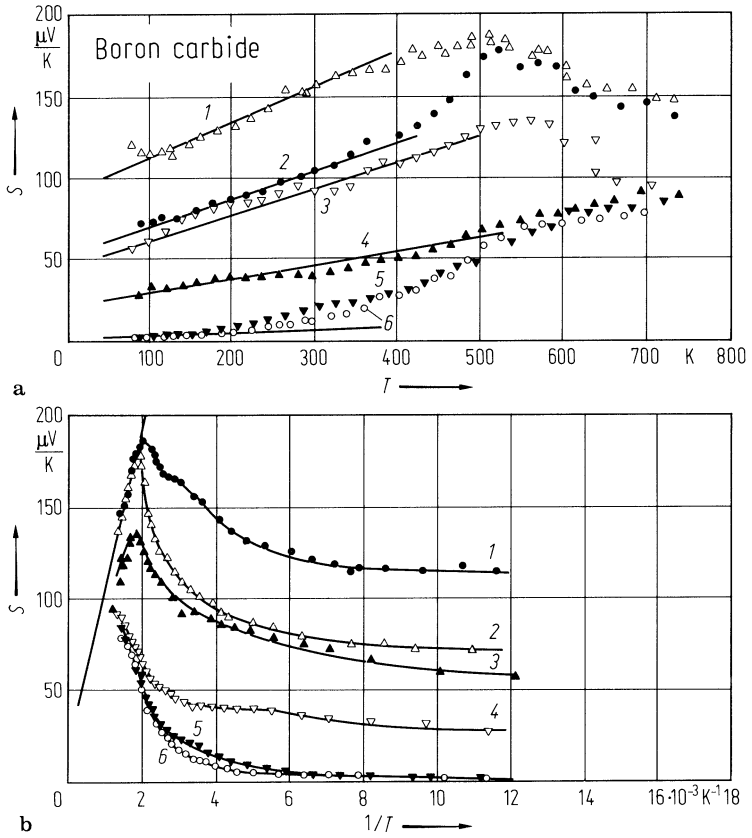

Fig. 4.

Boron carbide. Hall coefficient vs. medium distance of the C atoms [81W2].

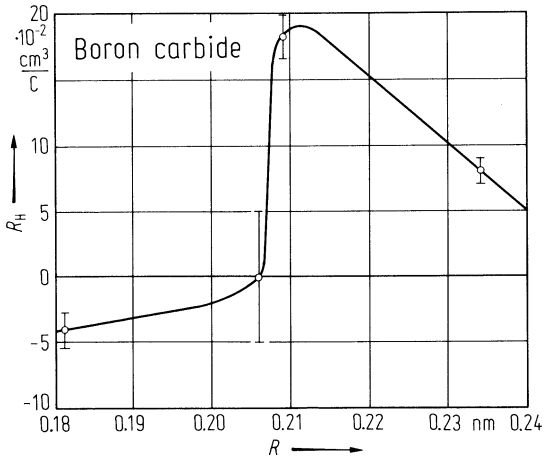

Fig. 5.

Boron carbide. Preliminary band scheme, which is compatible with the experimentally determined transition energies. The donor level has not yet been experimentally proved [98S, 99S3]. Energy values relative to the valence band edge for $B_{4.3}C$ at T = 300 K.

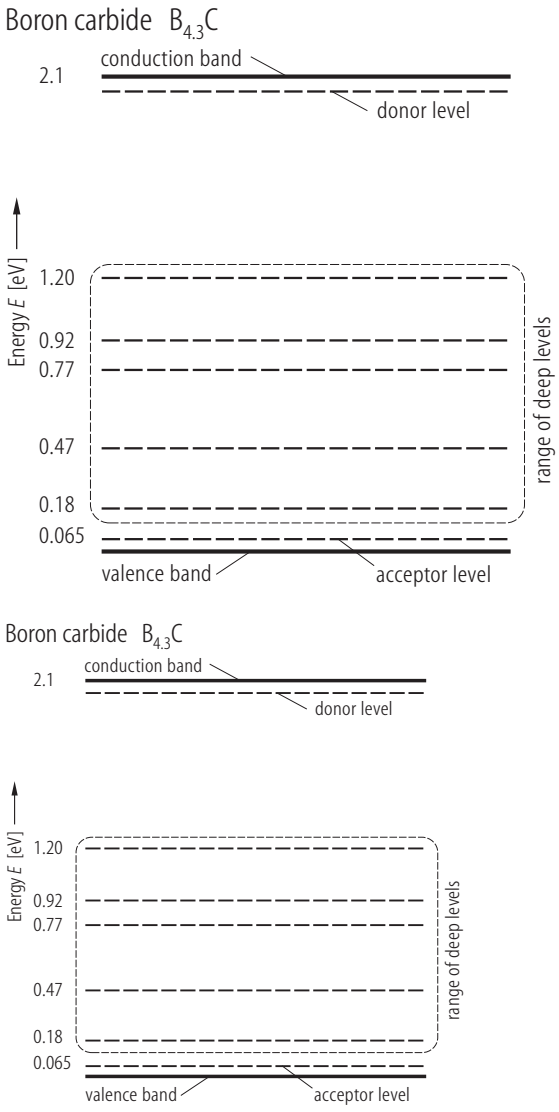

Fig. 6.

Boron carbide. Electrical conductivity for dc (closed symbols) and 10^{10} Hz (open symbols) vs. carbon concentration [93S].

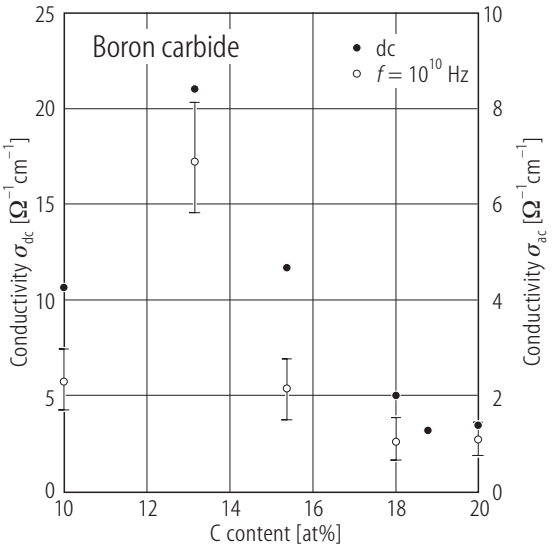

Fig. 7.

Boron carbide. Activation energy E_A of the electrical conductivity and the Peltier energy $E_s = e \cdot S \cdot T$ at 100 K vs. medium distance of the C atoms [80W, 81W3].

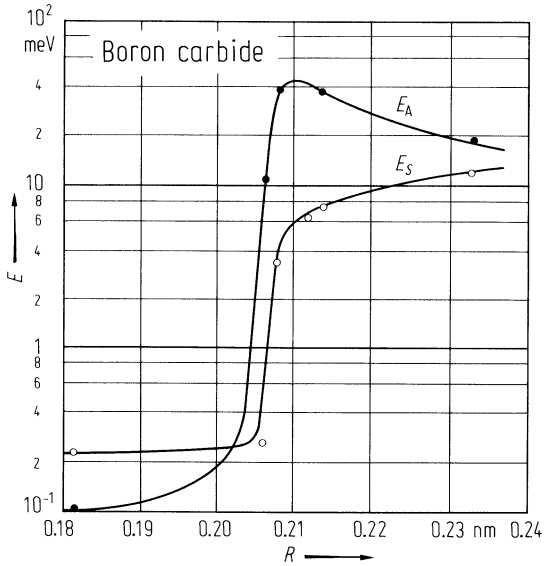

Fig. 8.

Boron carbide. Activation energy of the electrical conductivity of boron carbide of different composition vs. reciprocal temperature [80W, 81W3]. (Sample compositions: 1) $B_{12.94}C_{2.06}$; 2) $B_{12.35}C_{2.65}$; 3) $B_{12.28}C_{2.72}$; 4) $B_{12.13}C_{2.87}$; 5) $B_{12.01}C_{2.99}$; 6) $B_{10.6}C_{4.41}$; 7, 8) [70G2] unknown composition, accordingly analyzed measurements.).

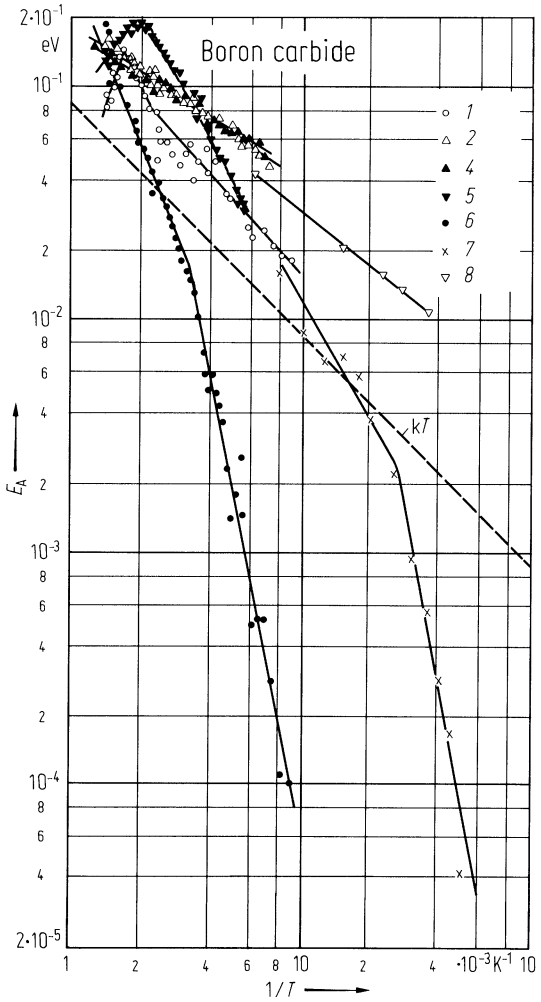

Fig. 9.

Boron carbide. Electrical conductivity vs. B/C relation and temperature [90W2, 94K3, 99W].

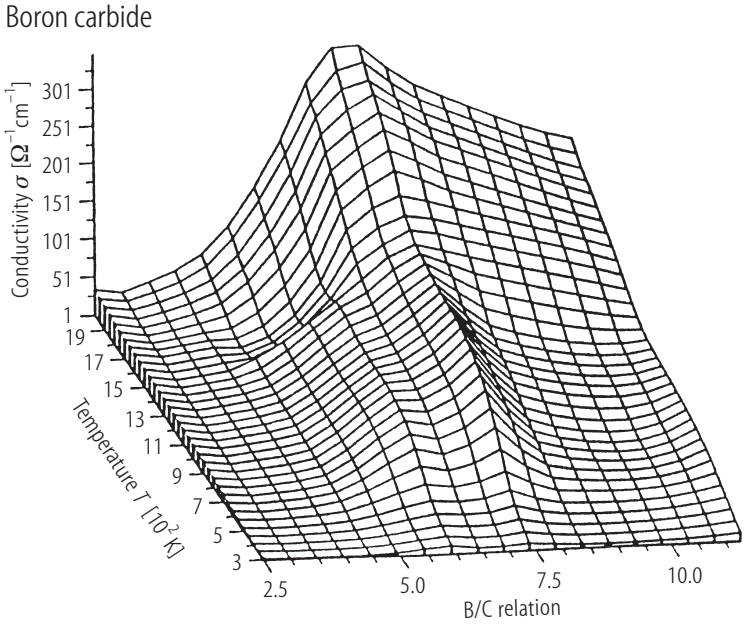

Fig. 10.

Boron carbide. Electrical conductivity of different compounds within the homogeneity range for temperatures between about 5 and 2200 K plotted according to Mott's law for variable-range hopping vs. $T^{-1/4}$ [99W].

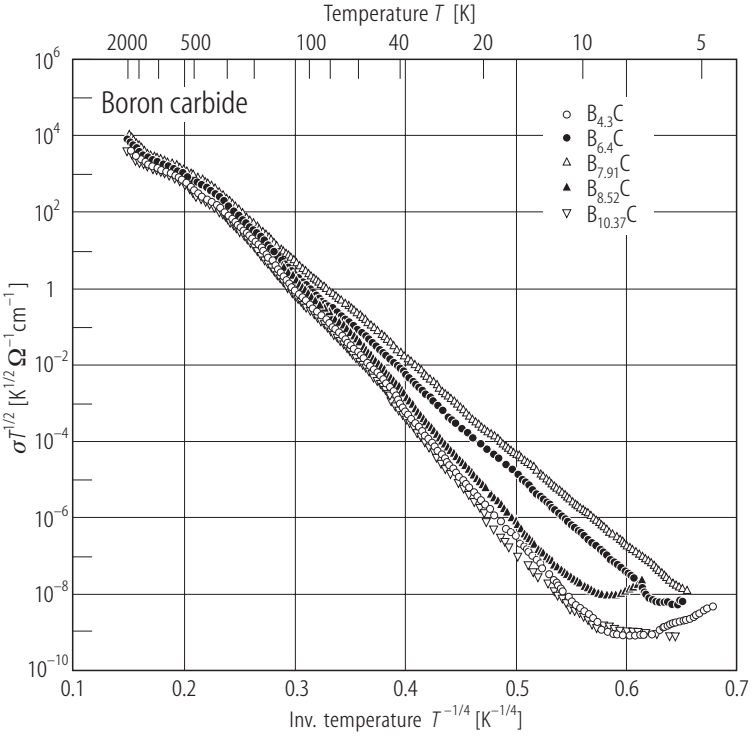

Fig. 11.

Boron carbide. **(a)** High temperature electrical conductivity vs. reciprocal T for (full circles) B_4C [86W1, 86W5, 87W4]; (open circles) B_4C, (open triangles) $B_{6.4}C$, (full triangles) $B_{10.37}C$ [90W2, 94K3, 99W]. **(b)** $B_{13}C_2$ (experimental results from [86W2, 87W4]).

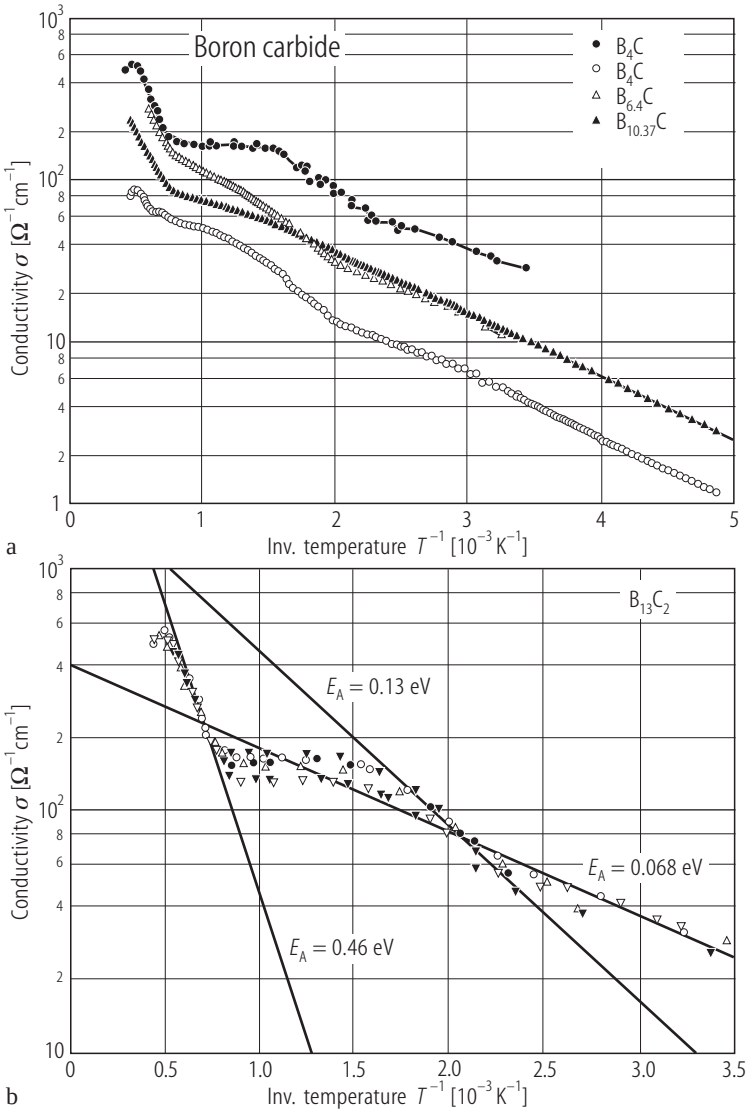

Fig. 12.

Boron carbide. Scaling behavior of the electrical conductivity of boron carbide, d log σ/dT vs. log(σ^{-1}) [99W]. Molten samples [80W, 81W3]: open squares, $B_{4.01}C$, open triangles up, $B_{4.23}C$, open circles, $B_{4.7}C$, open triangles down, $B_{6.3}C$; BARC sample [90N]: crosses, B_4C; hot-pressed/sintered samples [91W]: full triangles up, $B_{4.3}C$, pluses, $B_{6.2}C$, full triangles down, $B_{6.4}C$, full diamond, $B_{7.91}C$, full circles, $B_{8.52}C$, full squares, $B_{10.37}C$.

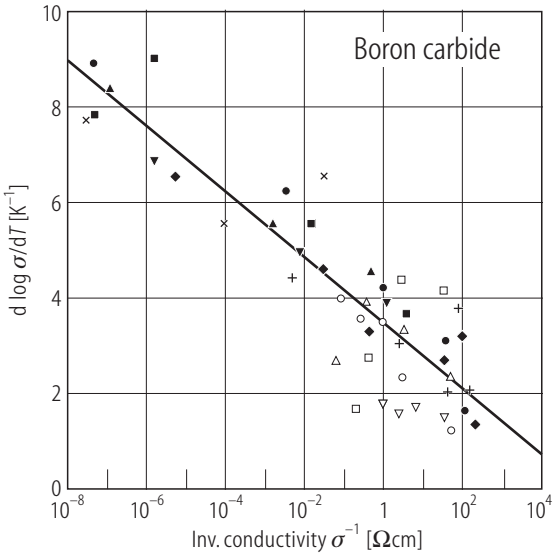

Fig. 13.

Boron carbide ($B_{\sim 4.3}C$) Anisotropy of the electrical conductivity; **(a)** $\sigma(\|c)$ **(b)** $\sigma(\perp c)$ vs. reciprocal T. Several single crystals grown by chance during the industrial production process (Elektroschmelzwerk Kempten). Since the production is aimed for the composition B_4C, the composition of the single crystals is expected not essentially to deviate from this composition. **(c)** anisotropy factor $\sigma(\|c)/\sigma(\perp c)$ vs. $10^3/T$ [86W4].

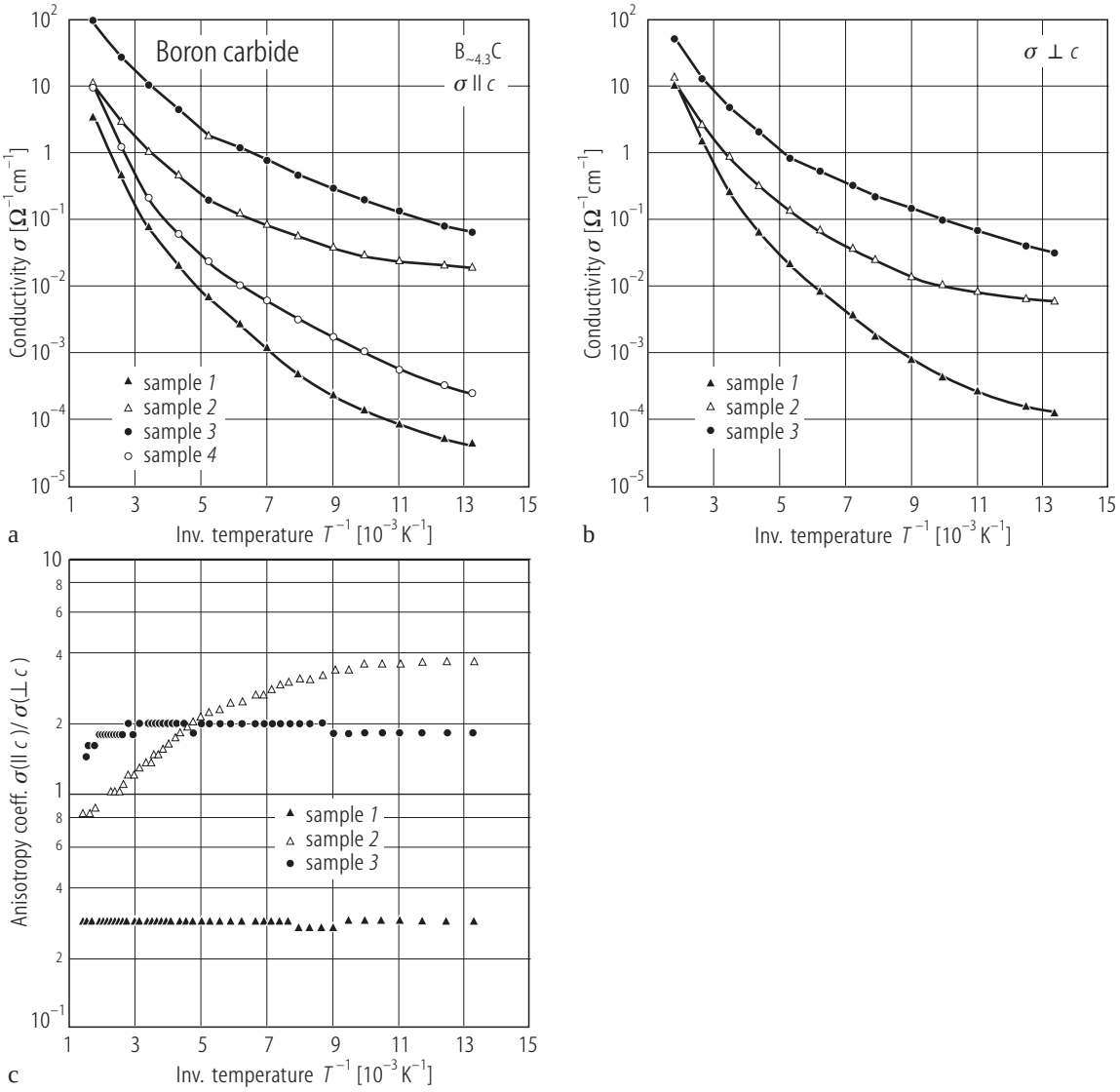

Fig. 14.

Boron carbide (B_4C, B_9C). Electrical conductivity vs. pressure [85S].

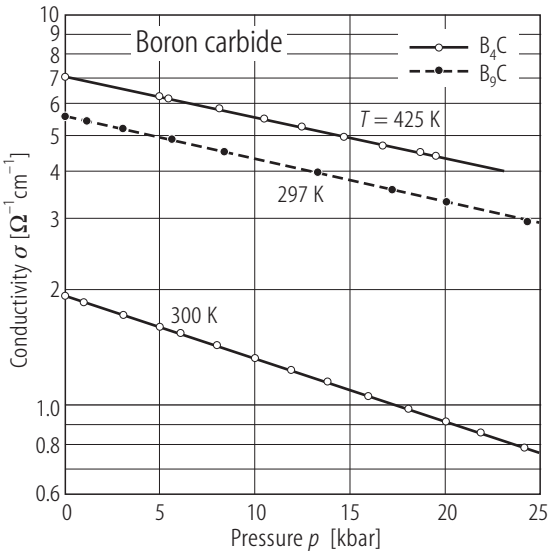

Fig. 15.

Boron carbide (B_4C). Temperature dependence of the electrical conductivity; σT vs. reciprocal T for different pressures [85S].

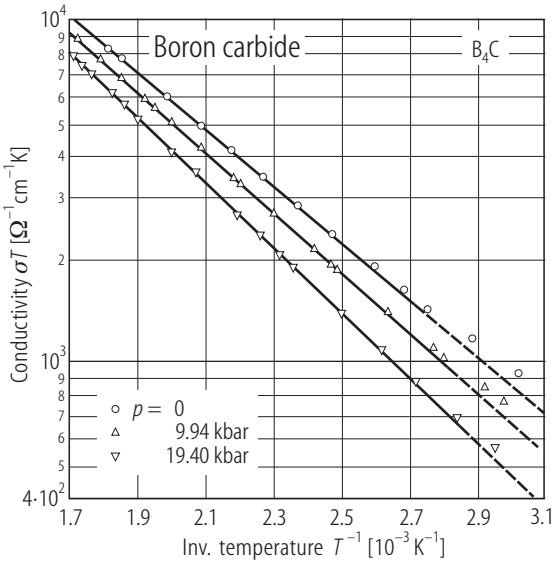

Fig. 16.

Boron carbide. $I(V)$ for a single crystal (approximately $B_{4.3}C$) [86W4].

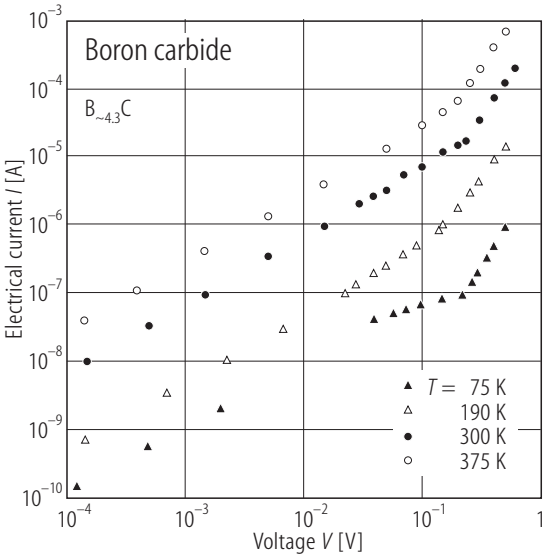

Fig. 17.

Boron carbide. Dependence of the dc and high frequency electrical conductivity of the carbon content. Open circles, dc conductivity σ at 450K [90W2] open triangles down, dc conductivity σ at 300K [80W, 81W3], open squares, dc conductivity σ at 2000K [90W2], open triangles up, dc conductivity σ at 450K [86W1], full circles, $\omega_p{}^2$ proportional to the density of Drude-type carriers at 450 K [97K]. Fig. from [97S, 98W].

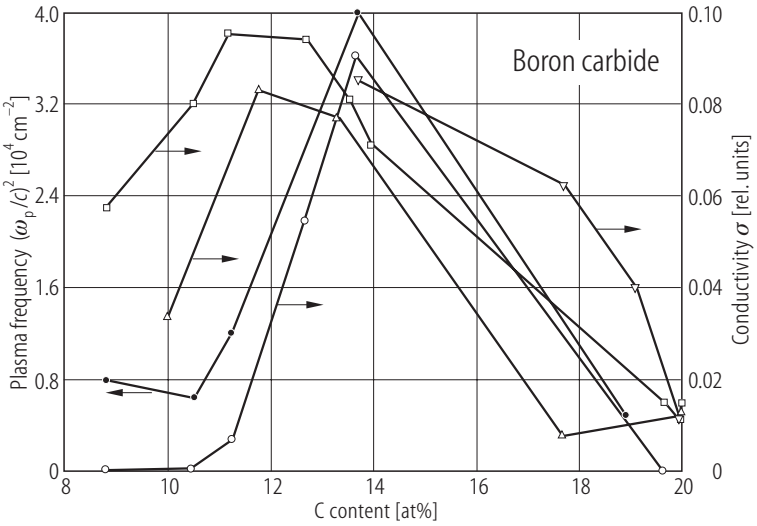

Fig. 18.

Boron carbide. Minimum hopping rate γ_m (left) and dc conductivity (right) vs. reciprocal T for B_4C, $B_{4.3}C$, $B_{13}C_2$ [91Z].

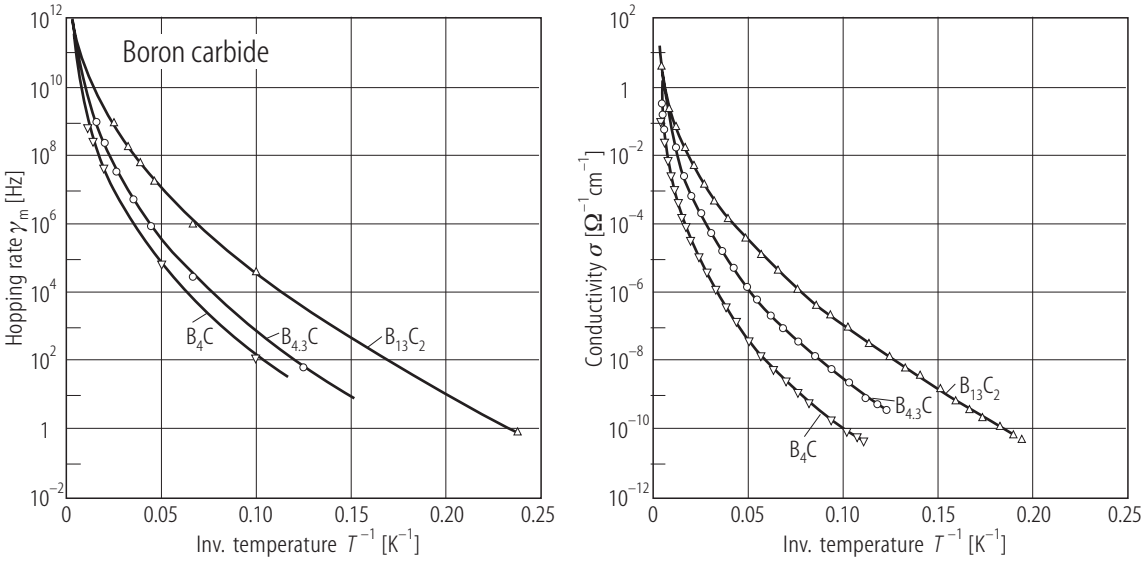

Fig. 19.

Boron carbide (B_9C). Effect of thermal cycling on **(a)** the resistivity and **(b)** the thermoelectric power [86W5].

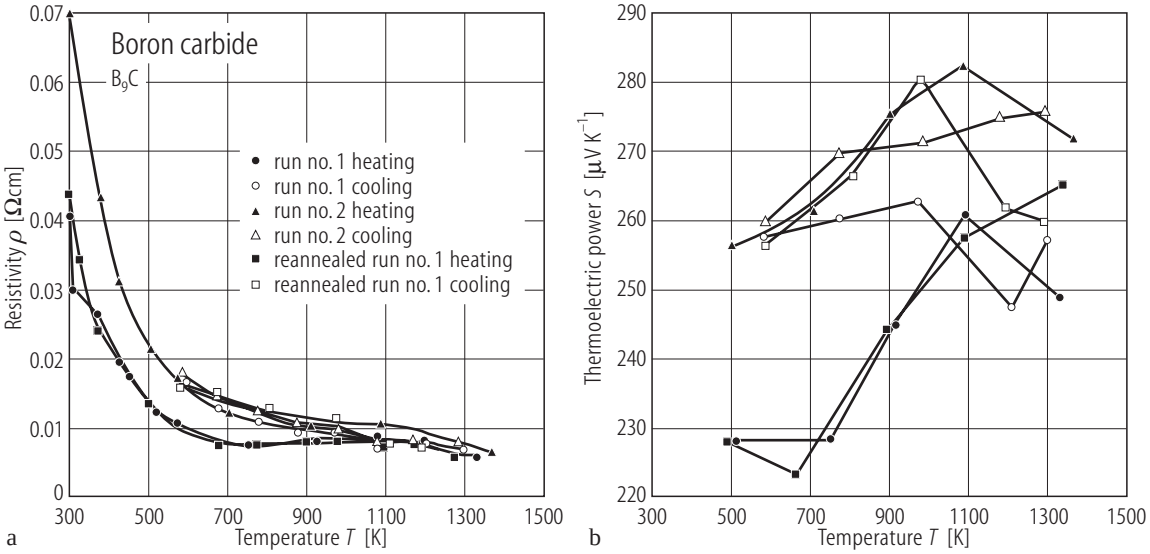

Fig. 20.

Boron carbide :P. ac conductivity between 10^3 and 10^6 Hz vs. temperature. P doped boron carbide (x = 0.05 in the assumed compound $(B_{11}C)(CBC)_{1-x}(PB)_x$) compared with undoped boron carbide (18 at% C, dashed lines) vs. temperature [93A]. $\sigma_0 = 1\ \Omega^{-1}cm^{-1}$.

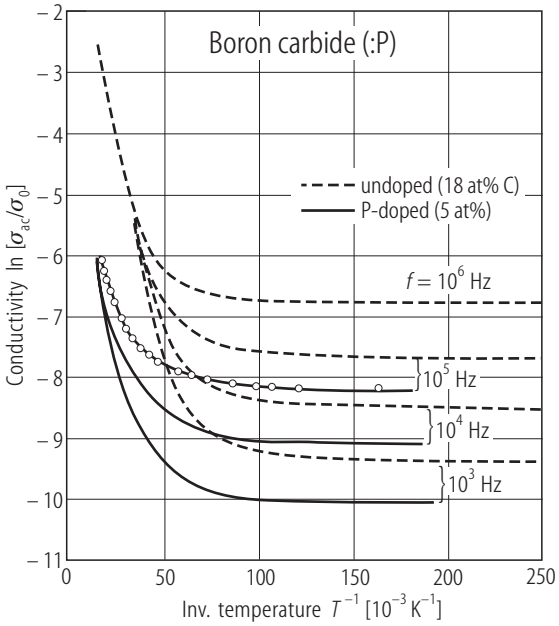

Fig. 21.

Boron carbide. Electrical conductivity for dc (closed symbols) and 10^{10} Hz (open symbols) vs. carbon concentration [93S].

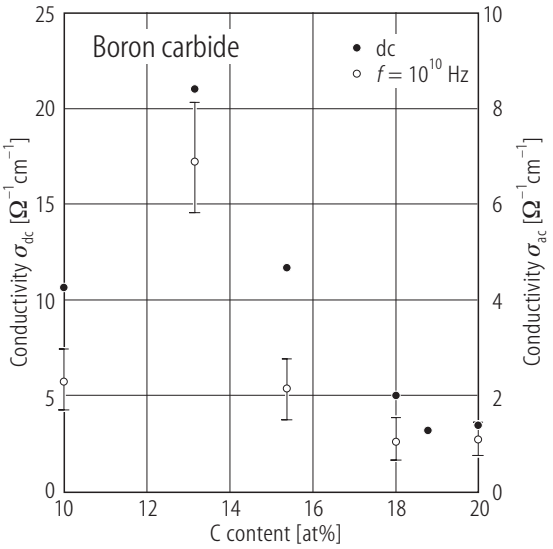

Fig. 22.

Boron carbide Frequency dependence of the ac conductivity of $B_{4.5}C$ at T = 4 K and B_9C at T = 4, 10, and 15 K. Insert: temperature dependence of the power-law dependence on frequency for B_9C [93S]. $\sigma_{ac} = \sigma(\omega) - \sigma_{dc} \cong A_1\omega^s$. Power law exponent s = 0.85...0.90 at 4K for the various compositions studied. These values are strongly dependent on temperature, with indications that s $\rightarrow$ 1 as $T \rightarrow$0 K.

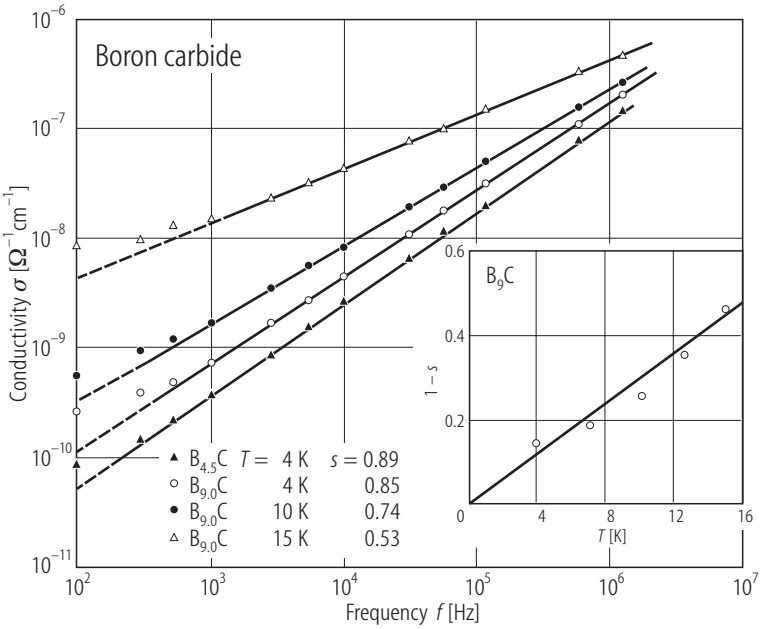

Fig. 23.

Boron carbide. Temperature dependence of the electrical conductivity of **(a)** $B_{4.5}C$ and **(b)** B_9C for frequencies between 10^3 and 10^6 Hz [93S].

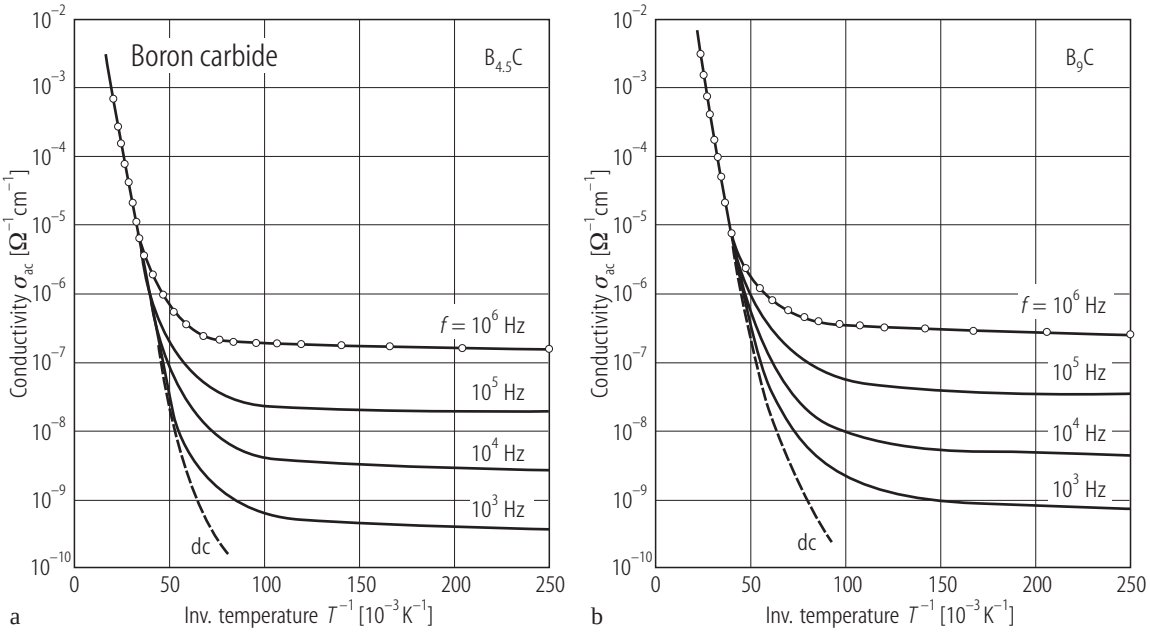

Fig. 24.

Boron carbide. log-log plot of the frequency dependence of the electrical conductivity at various temperatures for **(a)** $B_{4.3}C$) and **(b)** $B_{13}C_2$ [91Z].

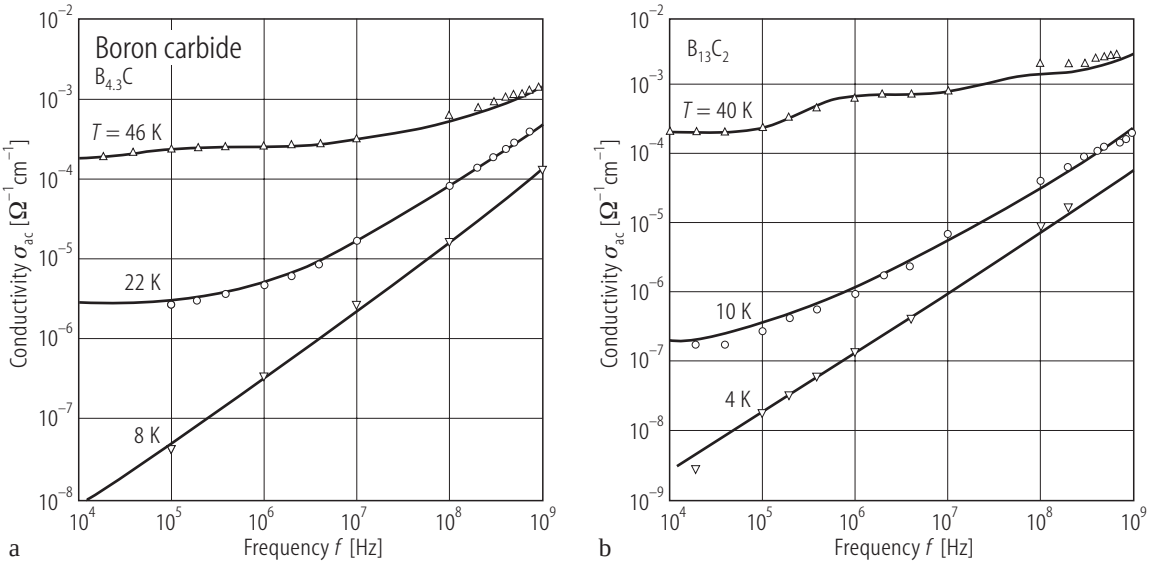

Fig. 25.

Boron carbide ($B_{1-x}C_x$). log-log plot of the absolute conductivity vs. frequency at 4.2 K. Solid line $\sigma_{ac} = \sigma_0 \omega^{0.9}$.The prefactor σ_0 is 6 times lower at the composition x ≈ 0.13 (2 samples) than x = 0.2 (4 samples) [86K].

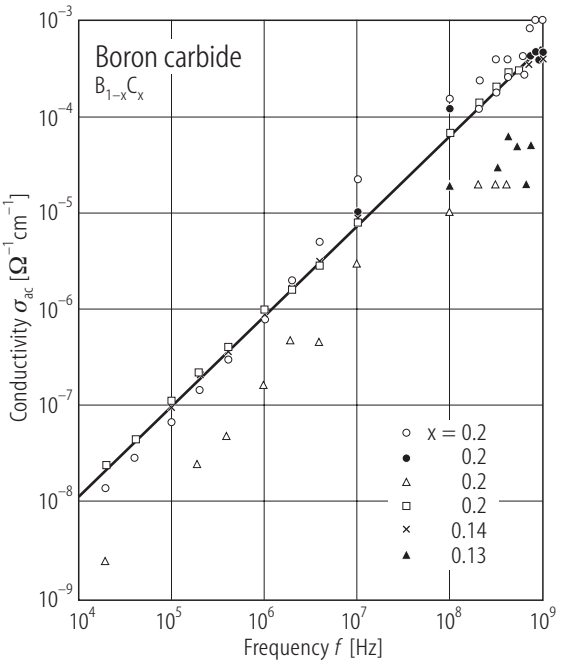

Fig. 26.

Boron carbide (B_4C). Electrical conductivity vs. reciprocal temperature for dc, 10^5, 10^6, 10^7, 10^8 and 10^9 Hz [86K].

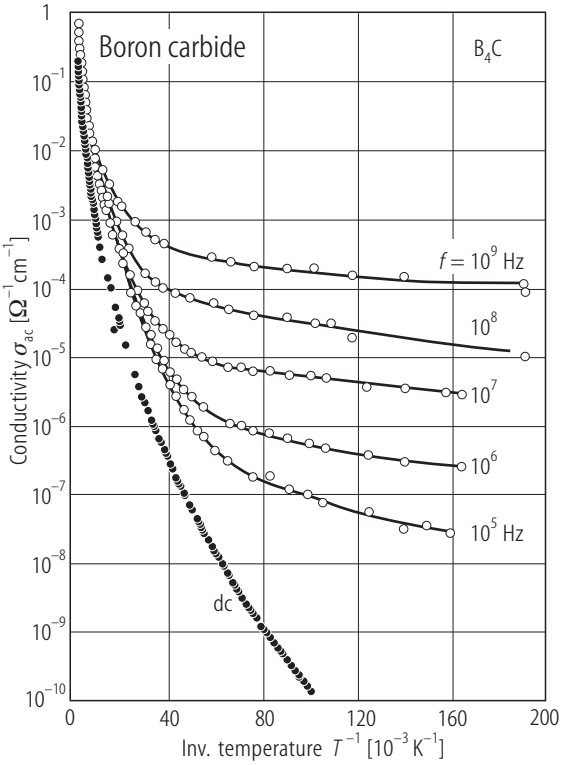

Fig. 27.

Boron carbide. (unknown composition; approximately $B_{12}C_3$) IR reflectivity vs. wavenumber. The sample dependent increase of R to wavenumbers < 350 cm^{-1} is attributed to the plasma resonance of free carriers [79B1].

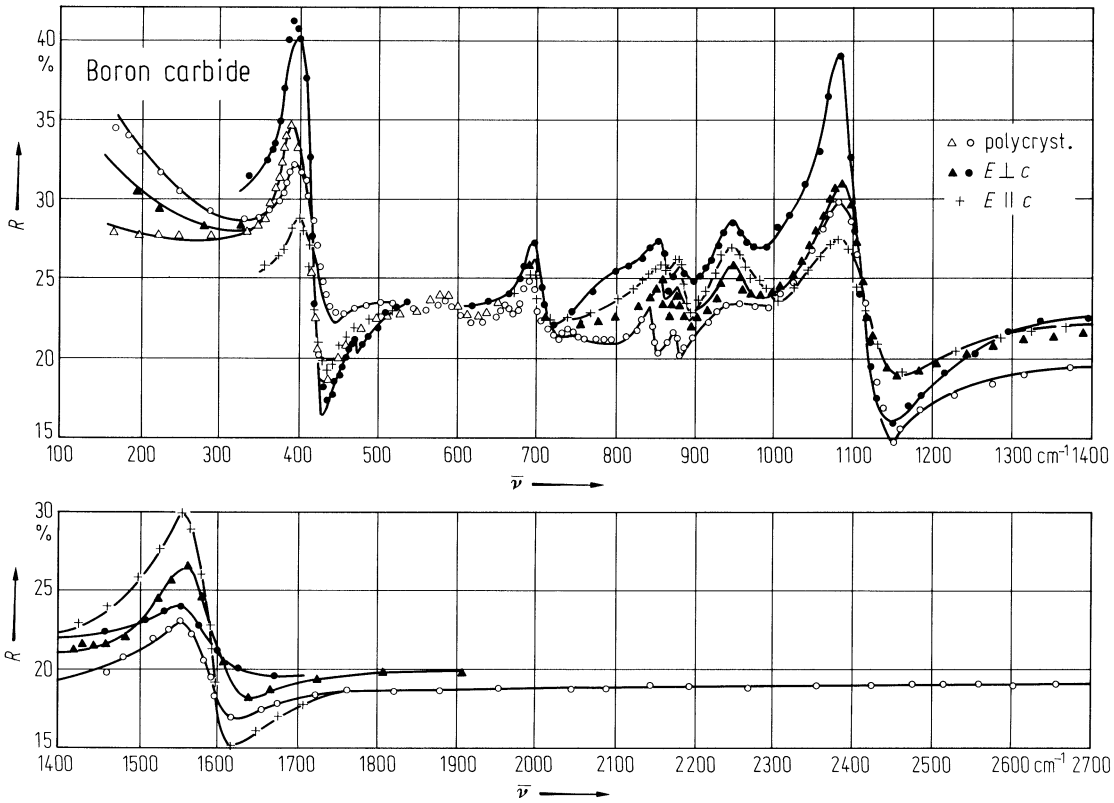

Fig. 28.

Boron carbide. Density of delocalized holes vs. reciprocal T derived from the dynamical conductivity of $B_{6.3}C$ and $B_{7.91}C$ (optical spectra) [98S, 99S1] compared with the Hall densities determined from Hall effect and magnetoresistance of $B_{4.3}C$ single crystals [85W, 87W3]. and compared with model calculations (i) taking the density of unoccupied atomic sites in the structure into account (full line) and (ii) based on an ideal structure without vacancies (broken line) [98S, 99S1].

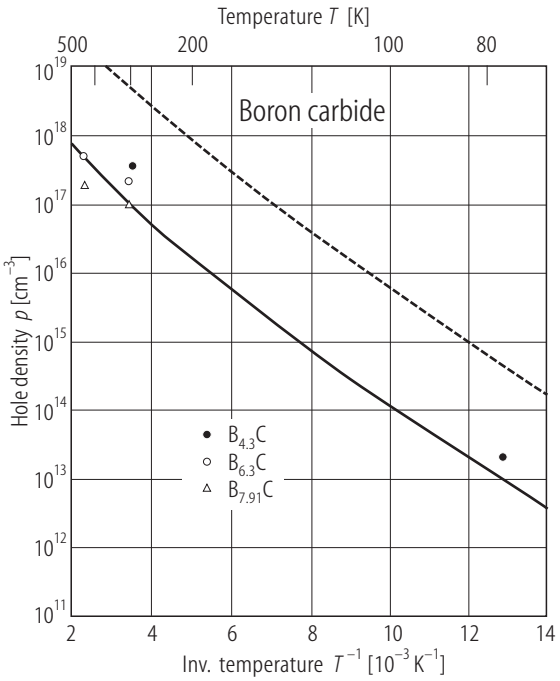

Fig. 29.

Boron carbide ($B_{10.37}C$). Difference $\Delta\alpha$ of the IR phonon spectra with and without optical excitation of carriers vs. wavenumber. Bottom tracing, IR phonon spectrum of boron carbide for orientation [97W].

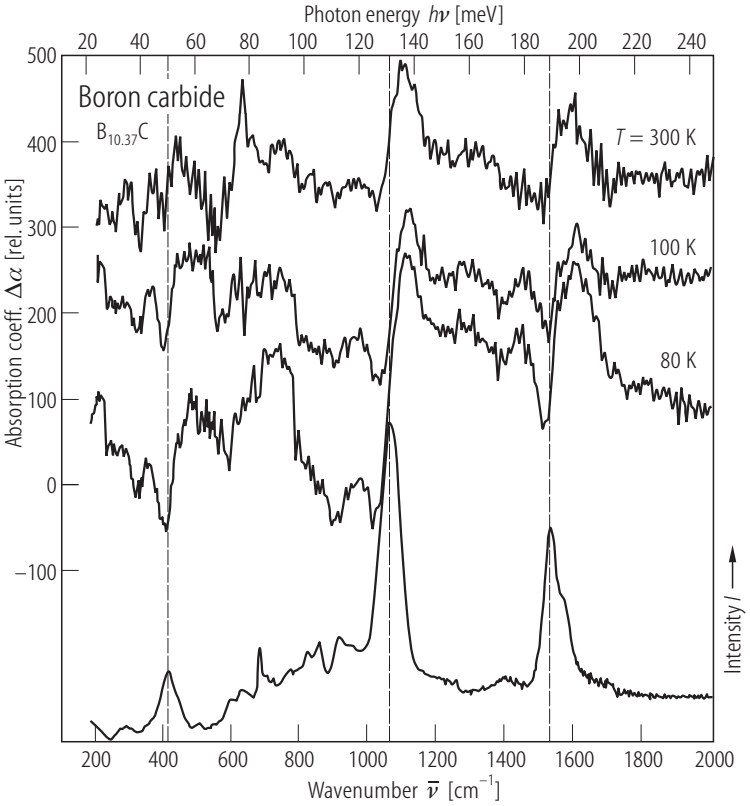

Fig. 30.

Boron carbide. Hall coefficient vs. medium distance of the C atoms [81W2].

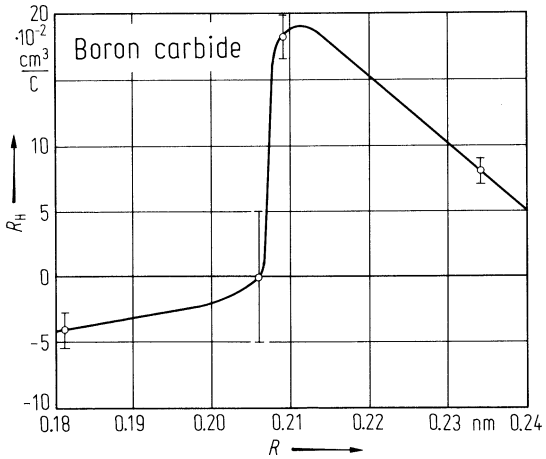

Fig. 31.

Boron carbide. Hall effect vs. carbon content for 15, 220, 400, 550 and 700 °C [86W5].

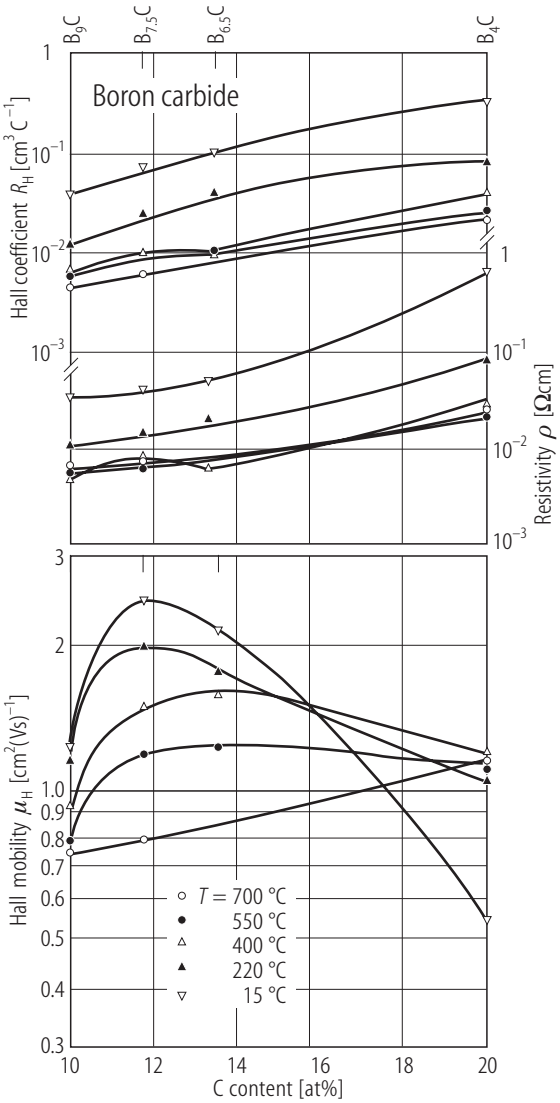

Fig. 32.

Boron carbide. Hall coefficient vs. reciprocal *T*. $B_{4.1}C$ (composition close to the carbon-rich limit of the homogeneity range), $B_{3.1}C$ (with excess carbon), $B_{8.3}C$ [90W2, 91W].

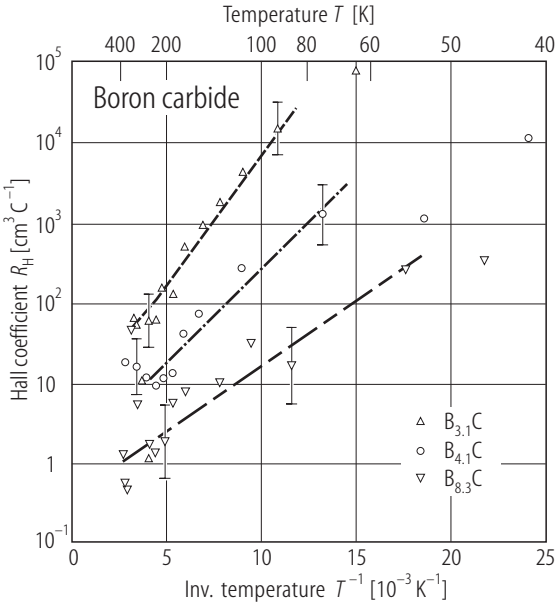

Fig. 33.

Boron carbide ($B_{13}C_2$). Temperature dependence of the Hall effect in a heating-cooling cycle [86W1, 86W5, 87W4].

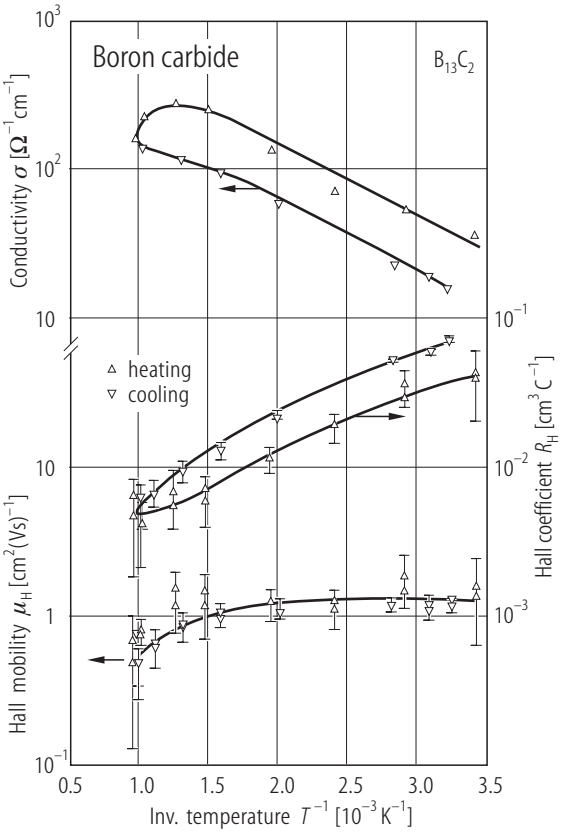

Fig. 34.

Boron carbide. Hall mobility of boron carbide vs. reciprocal temperature. (Open squares) probably ~$B_{4.3}C$ [70G1]; (full squares) B_4C; open triangles, (full triangles down), $B_{13}C_2$; (full triangles up), $B_{15}C_2$ [86W1, 86W5, 87W4]; (pluses) $B_{4.1}C$ (crosses) $B_{8.3}C$ [90W2, 91W]; (full circles) boron carbide with 16 at. % C and (open circles) with 18.2 at.% C [96C].

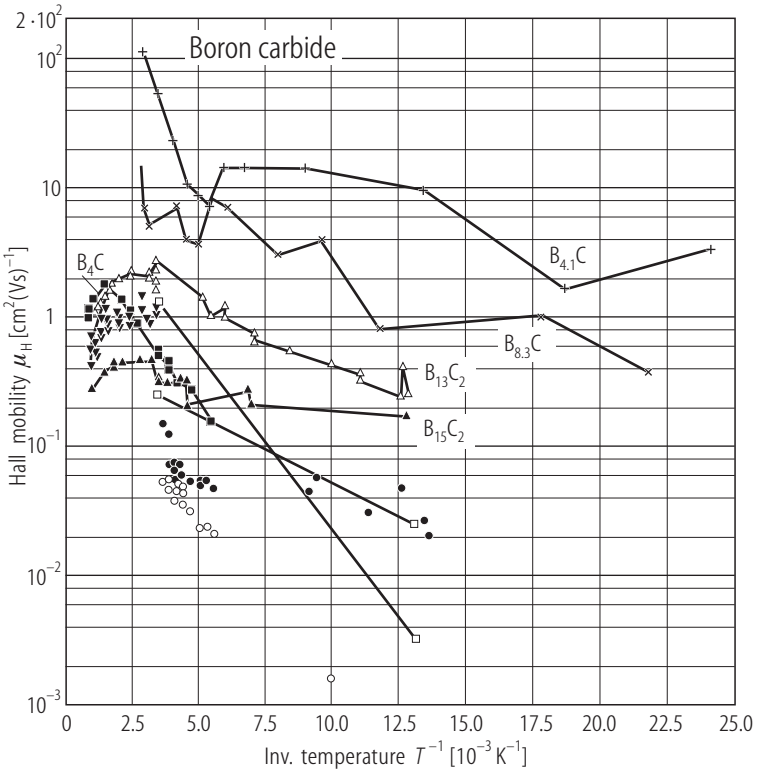

Fig. 35.

Boron carbide (CVD $B_{11}C$). Hall effect (Hall coefficient and Hall mobility) vs. reciprocal temperature [87C].

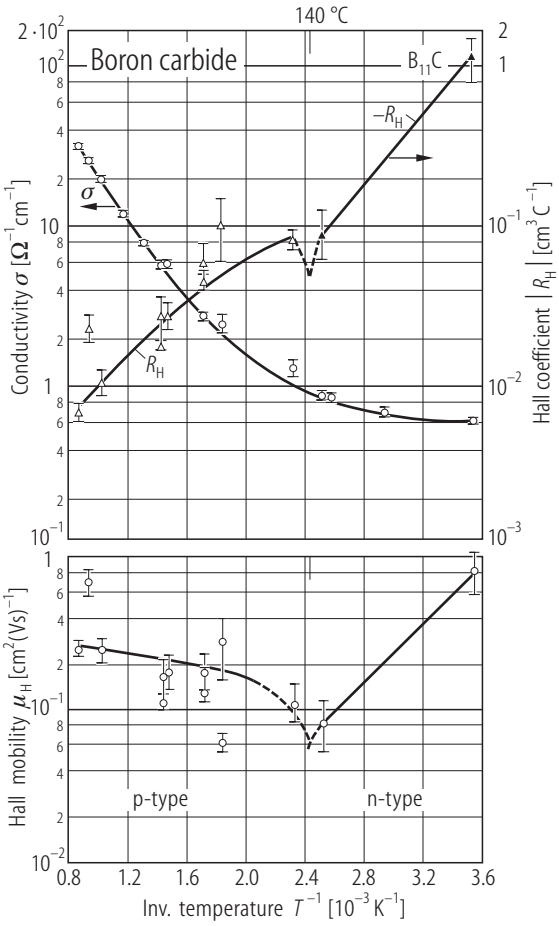

Fig. 36.

Boron carbide (CVD). Hall mobility vs. reciprocal temperature for $B_{4.00}C$, $B_{5.54}C$, $B_{6.57}C$ and $B_{9.62}C$ [94K1].

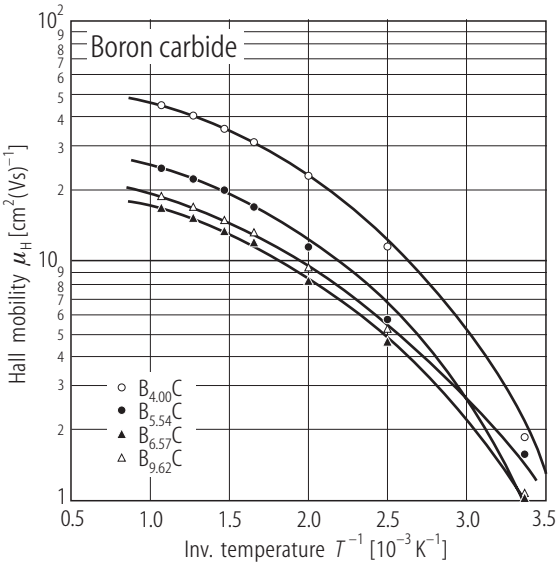

Fig. 37.

Boron carbide ($B_{4.3}C$). Magnetoresistance of a single crystal (occasionally obtained from industrial production in ESK) vs. squared magnetic induction at 77 and 290 K [87W3, 90W1, 91W].

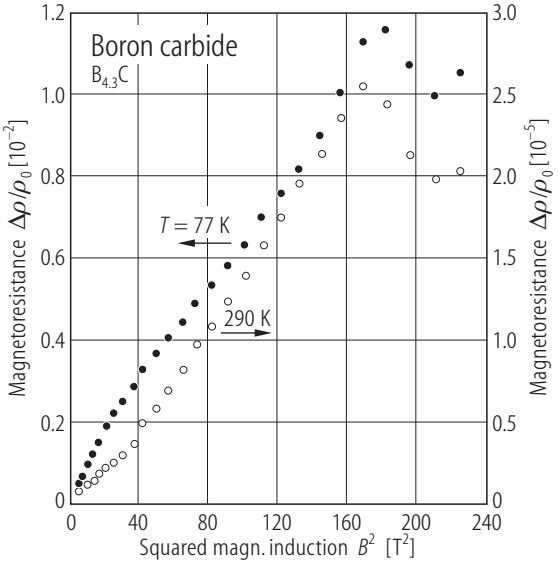

Fig. 38.

Boron carbide. Theory of the enhancement of the Seebeck coefficient through vibrational softening in consequence of a strong electron-phonon interaction. $F_{\text{vibrations}}(\Theta T) = [(\Theta/2T)/\sinh(\Theta/2T)]$ and $F_{\text{transport}}(\Theta/T) = (\Theta/T)[(\Theta/T)/\sinh(\Theta/T)]$, $\Theta = h\nu/k_B$ are the Einstein frequencies of the interacting phonons [98E, 99E].

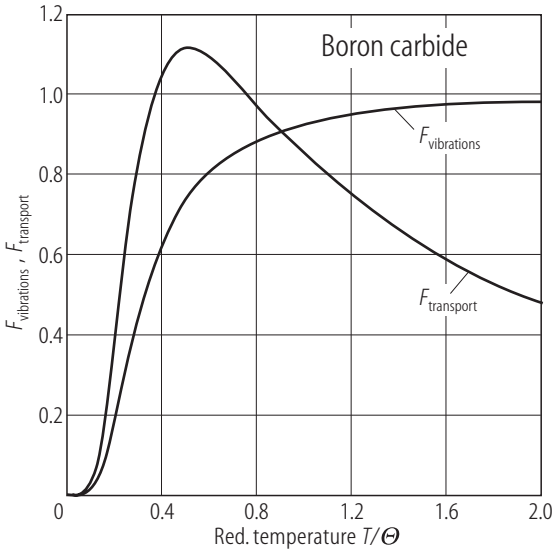

Fig. 39.

Boron carbide. Overview of typical results of the thermoelectric power as a function of temperature for various chemical compositions ($B_{4.1}C$, $B_{4.3}C$, $B_{6.2}C$, $B_{6.9}C$ [91W], $B_{4.3}C$ ($\|c$ and $\perp c$) [86W3, 86W4], see also [95W], B_4C, B_9C [86W1, 86W5], $B_{69}C_{11}Si$ [94W]; 10 % P-doped boron carbide [94A. „Conventional method“ means that thermocouples are used to determine the temperatures at both ends of the sample. If the thermocouples are not put into a sufficiently deep hole in the sample; the measurement can be considerably influenced by the heat flow through the wires of the thermocouple. In the „new method“ this source of error is avoided by deriving the temperatures from the electrical conductivity, that is separately measured with high accuracy.

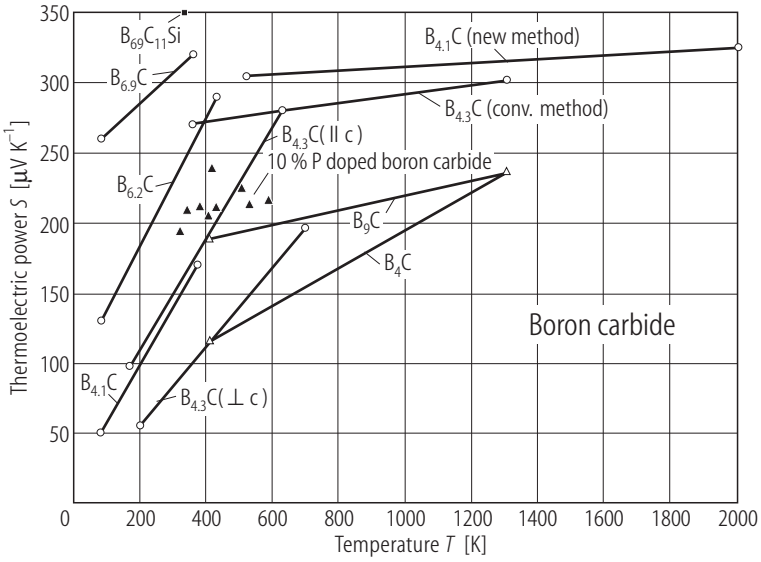

Fig. 40.

Boron carbide (CVD). Thermoelectric power vs. temperature for $B_{4.00}C$, $B_{4.95}C$, $B_{5.54}C$, $B_{6.57}C$, $B_{9.62}C$ and $B_{10.67}C$ [94K1].

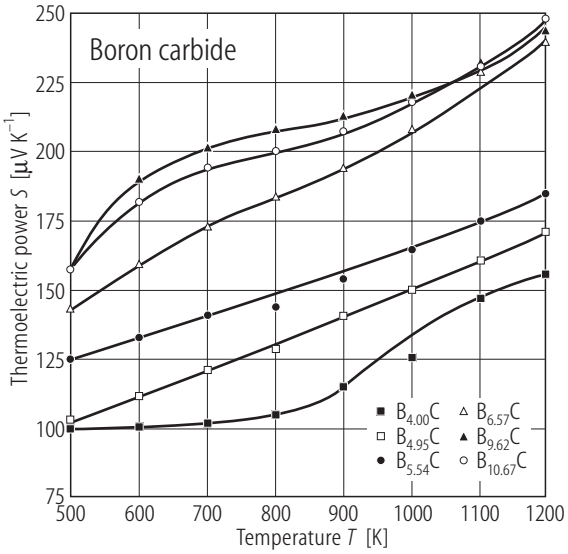

Fig. 41.

Boron carbide ($B_{6.5}C$). Temperature dependence of the thermoelectric power. Symbols, experimental data obtained in different equipments; solid line, calculated as the sum of contributions from $S_{vibrations}$ and $S_{transport}$ For the carrier-phonon interaction six low-level modes of 0.01 eV and one higher-energy mode of 0.06 eV were assumed. For details see [98A].

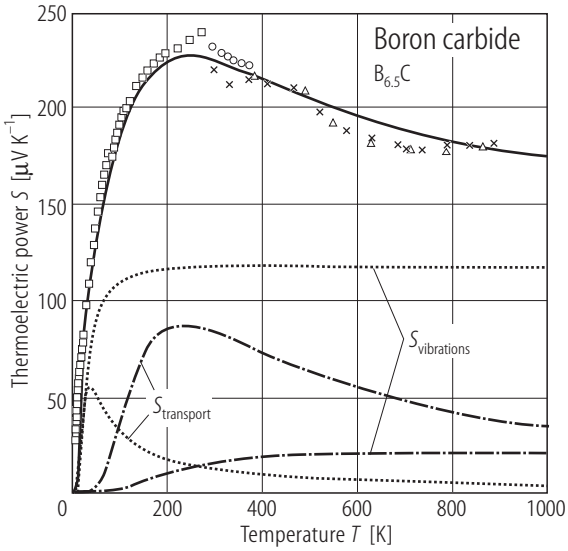

Fig. 42.

Boron carbide**.** Temperature dependence of the thermoelectric power. Circles and crosses, samples held between Cu anvils with Cu leads and type-K thermocouples; triangles and diamonds, samples held between graphite anvils with Pt leads and type-S thermocouples [98A]. Data for $B_{5.1}C$ are indicated by filled symbols.

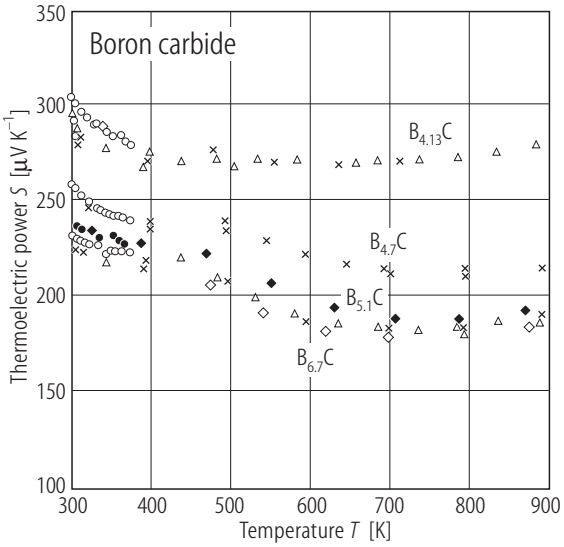

Fig. 43.

Boron carbide. Thermoelectric power vs. carbon concentration at T = 773 K [98A]. Solid line is a guide for the eye.